Global and Planetary Change 143 (2016) 100–117

Contents lists available at ScienceDirect

Global and Planetary Change

journal homepage: www.elsevier.com/locate/gloplacha

Regional hydrologic response to climate change in the conterminous United States using high-resolution hydroclimate simulations☆

Bibi S. Naz [a,b], Shih-Chieh Kao [a,b,*], Moetasim Ashfaq [a,c], Deeksha Rastogi [a,c], Rui Mei [a,c], Laura C. Bowling [d]

[a] Climate Change Science Institute, Oak Ridge National Laboratory, PO Box 2008, Oak Ridge, TN 37831, USA
[b] Environmental Sciences Division, Oak Ridge National Laboratory, PO Box 2008, Oak Ridge, TN 37831, USA
[c] Computer Science and Mathematics Division, Oak Ridge National Laboratory, PO Box 2008, Oak Ridge, TN 37831, USA
[d] Department of Agronomy, Purdue University, West Lafayette, IN 47907, USA

ARTICLE INFO

Article history:
Received 7 February 2016
Received in revised form 17 May 2016
Accepted 5 June 2016
Available online 16 June 2016

Keywords:
Hydroclimate change
Extreme events
CMIP5
RegCM4
VIC

ABSTRACT

Despite the fact that Global Climate Model (GCM) outputs have been used to project hydrologic impacts of climate change using off-line hydrologic models for two decades, many of these efforts have been disjointed — applications or at least calibrations have been focused on individual river basins and using a few of the available GCMs. This study improves upon earlier attempts by systematically projecting hydrologic impacts for the entire conterminous United States (US), using outputs from ten GCMs from the latest Coupled Model Intercomparison Project phase 5 (CMIP5) archive, with seamless hydrologic model calibration and validation techniques to produce a spatially and temporally consistent set of current hydrologic projections. The Variable Infiltration Capacity (VIC) model was forced with ten-member ensemble projections of precipitation and air temperature that were dynamically downscaled using a regional climate model (RegCM4) and bias-corrected to 1/24° (~4 km) grid resolution for the baseline (1966–2005) and future (2011–2050) periods under the Representative Concentration Pathway 8.5. Based on regional analysis, the VIC model projections indicate an increase in winter and spring total runoff due to increases in winter precipitation of up to 20% in most regions of the US. However, decreases in snow water equivalent (SWE) and snow-covered days will lead to significant decreases in summer runoff with more pronounced shifts in the time of occurrence of annual peak runoff projected over the eastern and western US. In contrast, the central US will experience year-round increases in total runoff, mostly associated with increases in both extreme high and low runoff. The projected hydrological changes described in this study have implications for various aspects of future water resource management, including water supply, flood and drought preparation, and reservoir operation.

1. Introduction

In the conterminous United States (CONUS), several studies based on modeling and observations show that climate change is resulting in the intensification of extreme precipitation and temperature (Diffenbaugh and Ashfaq, 2010), earlier snowmelt (Ashfaq et al., 2013; Abatzoglou, 2011; Mote, 2006), increases in the frequency and intensity of floods and droughts (Mahoney et al., 2012; Strzepek et al., 2010; Narisma et al., 2007; Frumhoff et al., 2007; Knox, 1993), and changes in the timing and magnitude of streamflow (Stewart et al., 2005; Milly et al., 2005). Such changes in hydrological conditions will have an immediate impact on local and regional communities and could have severe consequences for agriculture, property and human losses, energy production, and ecosystems. However, climate change impacts vary from region to region because of differences in geographical characteristics and local climate; thus hydrological response to climate change will be region-specific, depending on the dominant physical processes of a particular region (Hay et al., 2011). Therefore, it is necessary to understand the effects of projected climate change on regional hydrological cycles to support policy makers for more informed adoption and mitigation decisions. Additionally, understanding the spatial distribution of temporal variations of runoff is also important for water resource managers, because finer-scale modeling results can be used to infer practical water resource management decisions such as water allocation and reservoir operation.

☆ This manuscript has been authored by UT-Battelle, LLC, under Contract No. DE-AC05-00OR22725 with the US Department of Energy. The United States Government retains and the publisher, by accepting the article for publication, acknowledges that the United States Government retains a non-exclusive, paid-up, irrevocable, world-wide license to publish or reproduce the published form of this manuscript, or allow others to do so, for United States Government purposes. The Department of Energy will provide public access to these results of federally sponsored research in accordance with the DOE Public Access Plan (http://energy.gov/downloads/doe-public-access-plan).

* Corresponding author at: P.O. Box 2008, MS-6038, Oak Ridge, TN 37831-6038, USA.
E-mail address: kaos@ornl.gov (S.-C. Kao).

http://dx.doi.org/10.1016/j.gloplacha.2016.06.003
0921-8181/

Although a number of previous studies have investigated the impacts of climate change on water availability in the US, many of the studies focused on the western US (e.g., Rasmussen et al., 2014; Tohver et al., 2014; Hamlet et al., 2013; Ficklin et al., 2013; Barnett et al., 2004; Christensen et al., 2004; Payne et al., 2004; Stewart et al., 2005; Hamlet and Lettenmaier, 1999; Lettenmaier et al., 1999; Nash and Gleick, 1991; Milly et al., 2005; Seager et al., 2007; Seager and Vecchi, 2010; Mote et al., 2003). Comparatively few studies evaluated the future climate change impacts on the CONUS hydrology (e.g., Wolock and McCabe, 1999; Rosenberg et al., 2003; Thomson et al., 2005; Hay et al., 2011; Hagemann et al., 2013). Many of these past studies relied on hydrological outputs from Global Climate Models (GCMs) to drive one-way coupled hydrologic simulations. However, because of the coarser resolution of GCM grid cells, typically on the order of 150–200 km, hydrologic projections based on raw GCM outputs cannot be used directly for regional-scale water resource management studies. Thus, downscaling and bias-correction procedures are required to bring global climate change signals into watershed-scale hydrologic projections to support resource evaluation.

Different downscaling methods, such as bias-correction spatial disaggregation (BCSD; Wood et al., 2004), bias-correction constructed analogs (BCCA; Maurer et al., 2010), multivariate adaptive constructed analogs (MACA; Abatzoglou and Brown, 2012), and dynamical downscaling (e.g., North American Regional Climate Change Assessment Program; Mearns et al., 2012, 2013) have been used to support hydroclimate impact assessment in the CONUS (Hamlet et al., 2013; Christensen et al., 2004; Johnson et al., 2012; Glotter et al., 2014; Qiao et al., 2014; Takle et al., 2010; Elguindi and Grundstein, 2013; Bürger et al., 2011). In general, these methods either relied on statistical techniques that can be used to downscale temperature and precipitation from a large number of GCMs, or used computationally intensive regional climate models (RCMs) to downscale all hydroclimate variables in sub-daily time steps through physical relationships. Nevertheless, it should be noted that the effects of different downscaling methods on future hydroclimate projections have not been fully understood, and a consensus on the most suitable downscaling approach for future hydroclimate studies has yet to be reached (e.g., Chen et al., 2013).

In addition to the need for downscaling, the importance of fine-scale land surface modeling – particularly in topographically complex river basins, where topographic effects on hydrologic predictions are significant – has also been highlighted in a number of recent studies (Haddeland et al., 2002; Wood et al., 2011; Vano et al., 2014; Rasmussen et al., 2014). However, although these studies provide valuable watershed-scale hydroclimate information, the finer-resolution models have seldom been applied in a large study domain (e.g., regions or continents) mainly because of the data and computational limitations. In addition, given the differences in spatial and temporal resolution, model structure, and calibration approaches, the results from different finer-resolution studies cannot be inter-compared to provide a regionally coherent picture of future hydrology at a larger scale. To identify regions that are more sensitive to projected future climate changes (in terms of watershed-scale hydrologic response), a spatially and temporally consistent hydroclimate simulation framework is required.

To capture the fine-scale processes and to better understand regional and local hydrological responses to near future climate change, this study uses a hierarchal modeling framework to generate a large ensemble of computationally intensive hydroclimate projections for the evaluation of climate change impacts on regional hydrology across the entire CONUS. A hybrid dynamical and statistical downscaling is used for the refinement of GCM climate change signals for hydrologic simulation. While recent studies have demonstrated the added value of RCMs for impact assessment (Di Luca et al., 2012, 2013; Zhang et al., 2011; Chen et al., 2013; Elguindi and Grundstein, 2013), this study provides the most detailed (to date) characteristics of near-term regional and local hydroclimate projections using a high-resolution hydrologic model driven by ten dynamically downscaled and bias-corrected projections from an RCM. Here, we focus on understanding spatial and temporal hydrological change at the sub-basin scale in response to near-term future climate projections in the US. Changes in projected hydroclimate variables are further used to improve the understanding of the likely causes of changes in hydrological extremes, timing of peak runoff, and snow variables. Region-to-region variations in hydrological projection uncertainties are also examined. We present general methodology in Section 2, results in Section 3, discussion in Section 4, and conclusions in Section 5.

2. Methodology

2.1. Climate projections and downscaling

Using a hybrid downscaling approach (i.e., dynamical and statistical), coarser-resolution GCM outputs are first dynamically downscaled to 18 km resolution using the International Centre for Theoretical Physics Regional Climate Model version 4 (RegCM4) (Giorgi et al., 2012). Choice of RegCM4 is based on the extensive use of its earlier versions over the U.S. for high-resolution multi-decadal climate change simulations (e.g., Diffenbaugh et al., 2005, 2011; Mearns et al., 2012; Ashfaq et al., 2010; Mankin and Diffenbaugh, 2014). In total, ten Coupled Model Intercomparison Project phase 5 (CMIP5) GCMs under the Representative Concentration Pathway (RCP) 8.5 emission scenario (Table 1) are selected for downscaling. For each selected GCM, RegCM4 is forced at its lateral and lower boundaries every 6 h using atmospheric and sea-surface temperature fields from the GCM. The RegCM4 simulations are carried out at 18 km horizontal grid spacing with 18 vertical levels that cover a domain similar to that in Diffenbaugh et al. (2011). Each set of experiments consists of 41 years in the baseline (1965–2005) and 41 years in the near future (2010–2050) periods with the first year discarded for model spin-up.

The selection of GCMs is mainly based on data availability. Although more than 50 GCMs contributed to CMIP5, fewer than one-third archived three-dimensional atmospheric fields at a sub-daily timescale, which is necessary for dynamic downscaling. After balancing the resource limitations and the need for multimodel ensemble simulations (to better represent uncertainty across different GCMs), ten ensemble members, one from each different CMIP5 GCM, were selected. In addition, RCP 8.5 was selected, given that it is closest to the current observed trajectory. However, the performance and skills of each selected GCM are not specifically evaluated in this study.

In the second step of hybrid downscaling, the 18 km daily precipitation and maximum/minimum surface temperature from the RegCM4 simulation (both baseline and near future periods) are statistically bias-corrected to 1/24° (~4 km) resolution following the quantile-based bias correction approach, described in Ashfaq et al. (2010, 2013). The 1/24° (~4 km) resolution 1966–2005 monthly precipitation and temperature from the Parameter-elevation Regressions on Independent Slopes Model (PRISM) (Daly et al., 2008) are used as the historic observations to support bias correction. Given that some of the Pacific Northwest watersheds are located in Canada and are not covered by PRISM, the 1/16° (~6 km) resolution gridded observations from Hamlet et al. (2013) are spatially interpolated to 1/24° (~4 km) resolution over that region. Similarly, for watersheds in Mexico that flow into the Rio Grande River basin, the 1/8° (~12 km) resolution precipitation and temperature from Maurer et al. (2002) are spatially interpolated to a consistent 1/24° (~4 km) domain to support bias correction in this region.

For statistical bias-correction, the 18 km RegCM4 fields are first spatially interpolated using bilinear interpolation to the targeted 1/24° (~4 km) geographical grid. The average monthly values are then calculated for both baseline and future periods and used to compute quantiles (40 intervals) for each calendar month in each grid. Between the 1966–2005 observation and baseline simulations, a model bias

Table 1
List of ten global climate models (GCMs) selected for RegCM4 simulation.

No.	GCM name	Spatial resolution (latitude/longitude)	Emission scenario	Ensemble number
1	ACCESS1–0	1.24°/1.88°	RCP 8.5	r1i1p1
2	BCC-CSM1–1	2.81°/2.81°	RCP 8.5	r1i1p1
3	CCSM4	0.94°/1.25°	RCP 8.5	r6i1p1
4	CMCC-CM	0.75°/ 0.75°	RCP 8.5	r1i1p1
5	FGOALS-g2	3.00°/2.81°	RCP 8.5	r1i1p1
6	MIROC5	1.41°/1.41°	RCP 8.5	r1i1p1
7	MPI-ESM-MR	1.88°/1.88°	RCP 8.5	r1i1p1
8	MRI-CGCM3	1.13°/1.13°	RCP 8.5	r1i1p1
9	NorESM1-M	1.88°/2.50°	RCP 8.5	r1i1p1
10	IPSL-CM5A-LR	1.88°/3.75°	RCP 8.5	r1i1p1

correction function is established by mapping the corresponding quantiles in each calendar month and in each grid. Similarly, for the future period, the change in the magnitude of each quantile (quantile shift) is first calculated in each calendar month as a difference (future minus baseline) for minimum and maximum temperature and as a ratio (future divided by baseline) for precipitation. The bias-corrected future period quantiles are then generated by adding the quantile shifts to the bias-corrected baseline minimum and maximum temperature quantiles and by multiplying the quantile shift with the bias-corrected baseline precipitation quantiles. After the monthly values have been corrected, the total monthly adjustment is then evenly disaggregated to the daily time series (using degree adjustment for temperature and ratio adjustment for precipitation). An equal length for the observation, baseline, and future simulations (i.e., 40 years) was purposely selected so that additional interpolation between quantiles is not required. Readers are referred to Ashfaq et al. (2010, 2013) for further description and discussion of this bias-correction method. Given that most hydrologic models are highly sensitive to minor variations in meteorological forcings, several researchers have suggested performing statistical bias correction on the dynamically downscaled simulated precipitation and temperature before conducting hydrologic simulation for better accuracy and lower bias (Rojas et al., 2011; Muerth et al., 2013; Ashfaq et al., 2010; Ahmed et al., 2013).

Since our ensemble is restricted to ten GCMs and one RCM, we examine their representativeness compared to other CMIP5 members in Fig. 1. For comparison, 97 statistically downscaled climate projections under four emission scenarios (RCPs 2.6, 4.5, 6.0, and 8.5) were obtained from the BCSD data archive (Brekke et al., 2013). The average percentage change in precipitation and degree change in temperature from the 1966–2005 baseline to the 2011–2050 future period for the entire CONUS are calculated annually and for four seasons, including winter (DJF, December–January–February), spring (MAM, March–April–May), summer (JJA, June–July–August), and autumn (SON, September–October–November). The ensemble median of the 97 BCSD downscaled

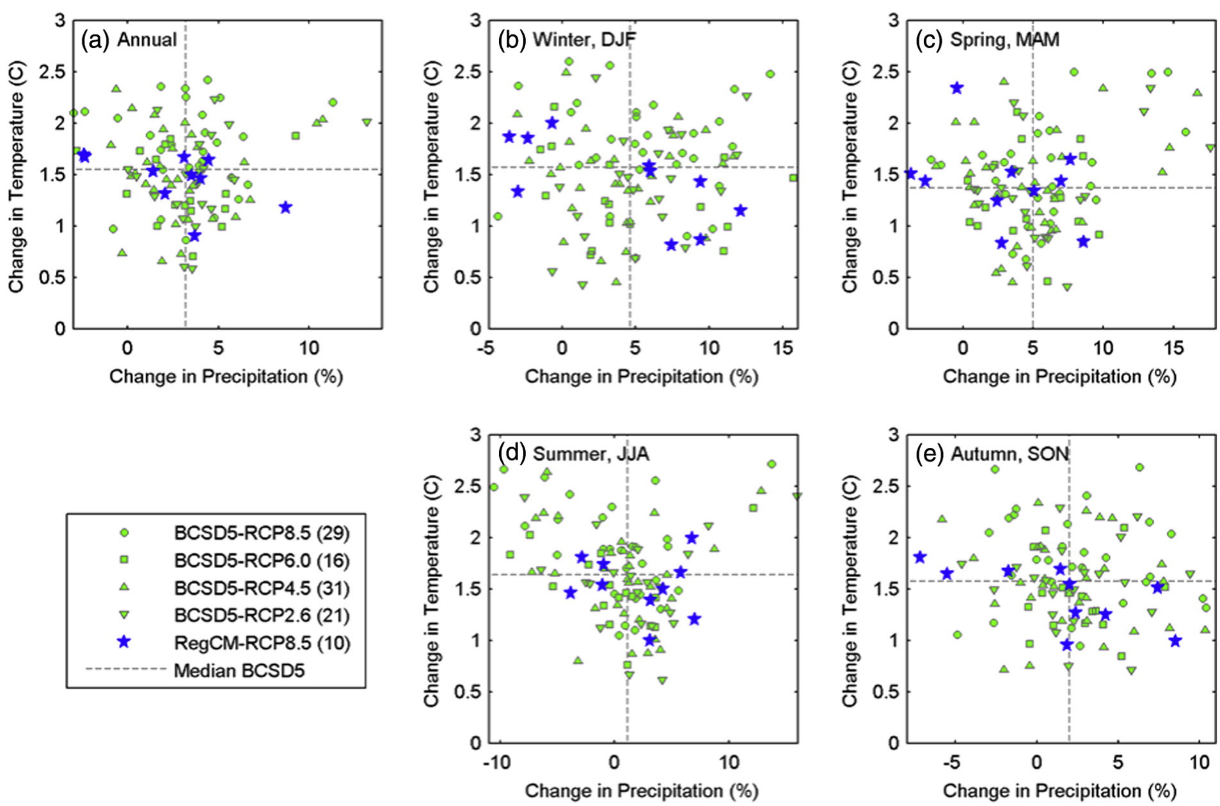

Fig. 1. Scatter plots of annual and seasonal temperature and precipitation changes for 97 statistically downscaled CMIP5 Global Climate Model projections under four emission scenarios (RCP 2.6, 4.5, 6.0, and 8.5; green symbols) plotted against the ten bias-corrected RegCM4 simulations (blue symbols) selected for this study. Change is defined as the degree change of national average temperature (°C) and percentage change in national average precipitation (%) from the 1966–2005 baseline to the 2011–2050 future periods. The 97 climate projections were obtained from the bias-correction spatial disaggregation (BCSD) data archive (Brekke et al., 2013).

projections is marked by a dashed line (Fig. 1). All models project a consistent increase in temperature ranging from +0.4 to +2.7 °C, and a change in precipitation ranging from −7 to ~ +12% with relatively large inter-model variability. Although our ten climate projections do not cover the full range of the projections, they spread around the median of the BCSD, suggesting that they do not exhibit bias in any one direction. It can also be seen that although the highest emission scenario is chosen, the ten simulations are not biased toward the warming side. This is because the difference among various emission scenarios becomes significant only after 2030 (Peters et al., 2013); hence, climate variability remains the main governing factor in the near-term 21st century projection period. Of ten RegCM4 simulations, only ACCESS1–0 projected a decrease in mean CONUS annual precipitation.

2.2. Hydrologic simulation

To study the hydrologic response to simulated climate change, we use the semi-distributed macroscale Variable Infiltration Capacity (VIC) hydrologic model (Liang et al., 1994, 1996; Cherkauer et al., 2003). The VIC model has been used widely for climate change impact assessment and can be used for either single basins (e.g., Christensen et al., 2004) or continental and global-scale studies (e.g., Vetter et al., 2015; Hagemann et al., 2013; Nijssen et al., 2001). VIC solves full water and energy balances (i.e., evaporation, energy fluxes, runoff, and baseflow) independently for each grid cell within a watershed. The infiltration and surface runoff are estimated using the variable infiltration capacity curve, which uses the soil moisture content of the upper two soil layers to approximate the spatial variability of surface saturation. The empirical Arno curve is used to generate base flow based on the soil moisture content in the bottom layer (Cherkauer et al., 2003). Every grid cell in the VIC model can account for subgrid variability in vegetation, precipitation, and topography, depending on selected options.

In this study, we implement VIC version 4.1.1 for the entire CONUS at 1/24° (~4 km) grid resolution with a 3 h time step. To fully preserve the spatial variability of precipitation from PRISM, the 1/24° (~4 km) grids are in the same configuration with PRISM (with the northern boundary extending to 53° N to cover the entire Columbia River basin on the Canadian side). At a higher spatial resolution, the VIC model may provide more detailed descriptions of topography, land uses, and soil types as well as hydro-meteorological forcing to capture the spatial variability in major runoff producing processes, particularly in the mountainous regions. However, since the VIC model does not consider horizontal water and energy exchange between grid cells, additional errors could be introduced at higher spatial resolution in areas where the horizontal exchange of water is more significant relative to the surface process. Although there have been few recent studies that implemented the VIC model at 1/16° (~6 km) resolution (e.g., Livneh et al., 2013, 2015; Hamlet et al., 2013; Tohver et al., 2014), the tradeoff between VIC model resolution and the simplification of horizontal water and energy exchange will require in-depth exploration in a future study.

To account for subgrid variability in topography and precipitation, five elevation bands are used within each grid cell. Pre-organized VIC input data with preliminary calibration over the entire CONUS were obtained from Oubeidillah et al. (2014). For the control run in the historic period (1980–2012), the VIC model was forced with the Daymet dataset (Thornton et al., 1997) and calibrated for the 2107 US Geological Survey (USGS) eight-digit hydrologic subbasins (HUC8) (Oubeidillah et al., 2014). The VIC model was calibrated for each HUC8 subbasin (Fig. 2) by matching the simulated monthly total runoff (surface runoff plus baseflow) with the observed monthly runoff from the USGS WaterWatch runoff dataset (Brakebill et al., 2011). WaterWatch runoff is a HUC8-averaged aggregated monthly runoff (mm/HUC8) derived from the USGS National Water Information System gauge observations. It has been used and discussed in some recent hydroclimate studies, including Ashfaq et al. (2013); Beigi and Tsai (2014), and Oubeidillah et al. (2014). Using the WaterWatch monthly runoff data for calibration

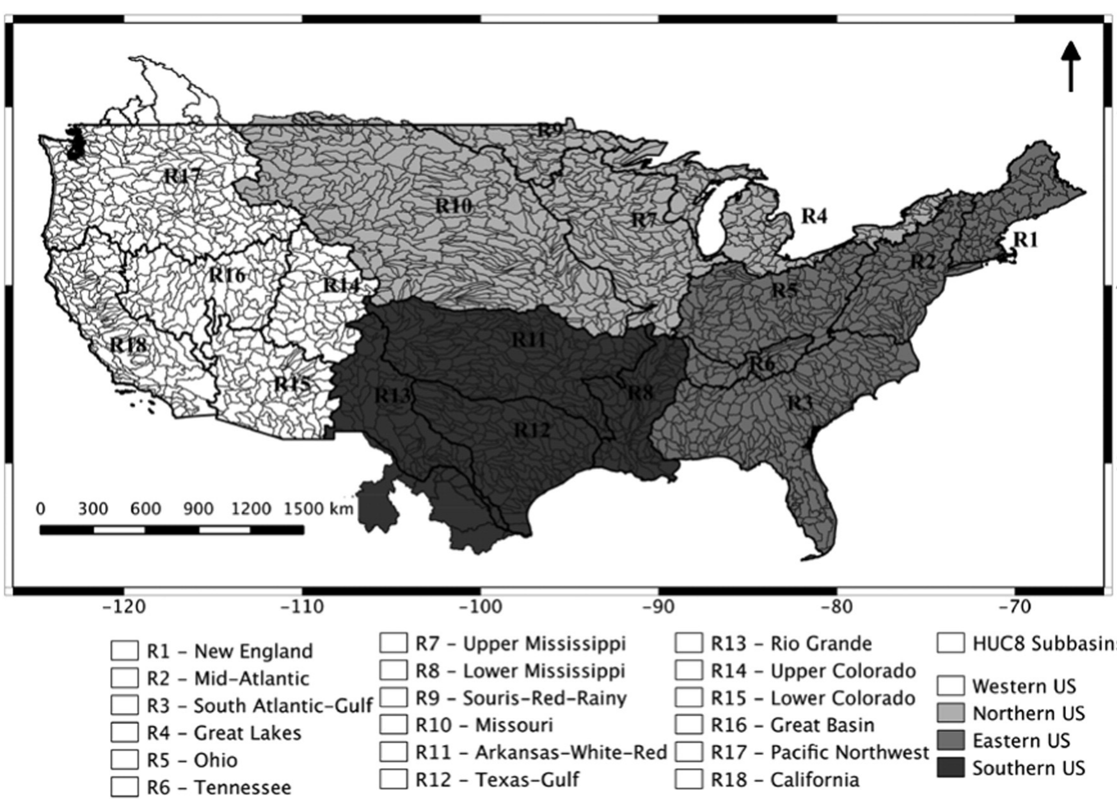

Fig. 2. Study area showing 18 hydrologic regions (HUC2) and hydrologic subbasins (HUC8) as defined by the US Geological Survey. The shaded areas represent the boundaries of the four regions used in the analysis. The numbers represent HUC2 identification codes.

allows homogenous application of the VIC model for all grid cells in the CONUS at the same spatial scale, as opposed to traditional calibration using streamflow routed to gauge locations, which requires parameter transfer to ungauged basins of various sizes. Nevertheless, since WaterWatch does not explicitly exclude gauges that are under flow regulation, the runoff estimates in HUC8s with significant historical human impairments could be biased. Further efforts can be made to replace the regulated gauge observations in WaterWatch with naturalized flow estimates to remove the effects of human influence for hydrologic model calibration. Readers are referred to Oubeidillah et al. (2014) for a detailed description of the VIC model setup, input parameters, and model performance for calibration and evaluation times. For upstream watersheds in Canada, runoff is computed by an approach similar to the USGS WaterWatch using only natural (unregulated) flow stations from the HYDAT Database (Environment Canada, 2014).

Based on the pre-organized VIC input data (Oubeidillah et al., 2014), we further enhance the model performance in areas where the model simulations tended to overpredict runoff, particularly in arid regions in the central US (mostly caused by underprediction of evaporation). Model enhancement includes (1) adjustment of vegetation parameterization (e.g., testing an alternative gridded monthly Leaf Area Index database from Myneni et al. (1997) in arid regions to reduce the overprediction of runoff, (2) bias correction of the Daymet forcing data with the PRISM dataset to account for the orographic precipitation effect, (3) use of five equal-area elevation bands in each VIC grid cell to account for subgrid topography for better snow simulation, (4) recalibration of the model to include the third soil layer depth in addition to the five calibrated VIC parameters (b_i, exp., $thick_2$, Ds, Ws) used in the previous model formulation, and (5) calibration and model evaluation for non-US regions that contribute to the downstream areas in the US (i.e., headwater basins in Canada and Mexico). The results from the improved model parameterization are shown in Fig. 3, which compares the observed versus simulated annual total runoff for each of the HUC8 subbasins for both the 1981–2000 calibration and 2001–2008 validation periods. The improved model shows a stronger linear correlation (0.969 in calibration period and 0.965 in validation period) between observed and simulated mean annual runoff compared with the Oubeidillah et al. (2014) model simulations (0.954 in calibration period and 0.940 in validation period). Whereas the improvement in overall correlation is small, the overprediction of runoff in arid regions (e.g., HUC8s with runoff of less than 500 mm/year) has been greatly reduced, which raises confidence in the projections of the potential climate change effects on arid regions such as Colorado and Missouri.

Using the calibrated VIC parameters, three set of simulations are conducted for the entire CONUS in this study:

- Control-run simulation: driven by 1981–2012 observed meteorology used for VIC calibration;
- RegCM4-baseline: driven by 1966–2005 bias-corrected daily precipitation, minimum and maximum temperature, and simulated surface wind speed from the ten RegCM4 ensemble members discussed in Section 2.1; and

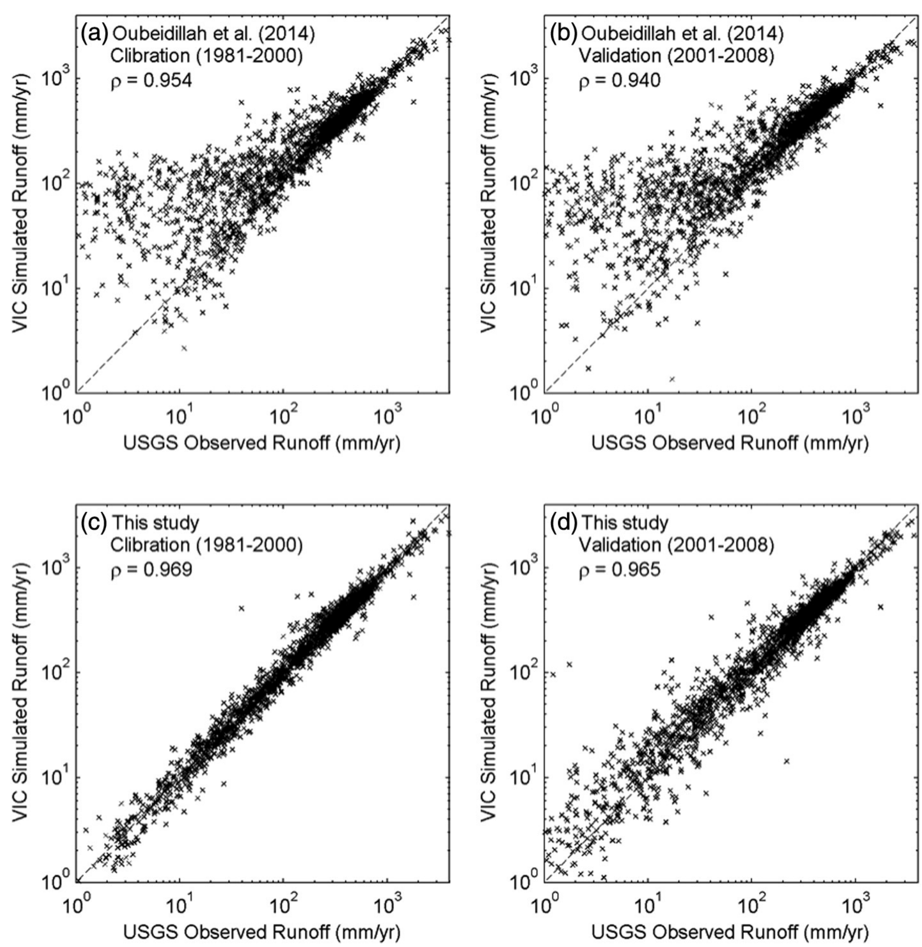

Fig. 3. Comparison of simulated (surface runoff + base flow) and observed (WaterWatch runoff data) annual total runoff for 1981–2000 calibration (left panels) and 2001–2008 validation (right panels) periods for each 8-digit hydrologic unit code (HUC8) subbasin using the Variable Infiltration Capacity (VIC) model setup of Oubeidillah et al. (2014) (upper panels) and this study (lower panels).

• RegCM4-future: the same as for the RegCM4-baseline, driven by 2011–2050 downscaled metrology.

2.3. Climate change indices

We use the following indices to evaluate changes in regional hydrologic response in the future period (2011–2050) relative to the baseline period (1961–2005).

(1) Seasonal percentage change (100% [future minus baseline]/baseline) in precipitation (P), evapotranspiration (ET) and total runoff (surface runoff plus baseflow; R), and absolute change (future minus baseline) in air temperature.
(2) Percentage change in high runoff is characterized by the 95th percentile (R95 — daily runoff equaled or exceeded 5% of the time) and low runoff by 5th percentile (R5 — daily runoff equaled or exceeded 95% of the time). A 30-day moving window is used to smooth out small variations in low runoff (similar to the approach used by Prudhomme et al., 2011).
(3) Mean annual change in April 1st SWE, number of snow-covered days, and maximum SWE. Calculations are based on those grid cells with annual average SWE of greater than 5 mm during the control-run simulation period. In areas such as the western US where snow is present for the entire winter season, April 1st SWE is a commonly used surrogate for the total seasonal accumulation. However, this index alone may not be representative of changes in the seasonal accumulation in the areas where snow is only intermittently present in the winter season such as the eastern US, therefore annual maximum SWE is also used to analyze projected changes in snowpack.
(4) Mean annual absolute change in the rain-to-precipitation ratio (i.e., ratio of liquid rain to precipitation) for the cold season (November to March).

Note that with the exception of snow variables (April 1st SWE, number of snow-covered days, annual maximum SWE, and rain-to-precipitation ratio), all other variables (T, P, ET, R, R95 and R5) are first aggregated to the HUC8 scale for each model run and simulation period. Future change between baseline and future simulations is calculated by first calculating the multimodel ensemble median of the ten baseline and future simulations, and then reporting the relative or absolute change in the median values. As shown in Fig. 2, the results are presented for each of the 18 two-digit hydrologic regions (HUC2) and for four mega regions including the eastern US (R1: New England, R2: Mid–Atlantic, *R*3: South Atlantic–Gulf, R5: Ohio, and R6: Tennessee), northern US (R4: Great Lakes, R: Missouri, R9: Souris–Red–Rainy, and R10: Upper Mississippi), southern US (R8: Lower Mississippi, R11: Arkansas-White-Red, R12: Texas–Gulf, and R13: Rio Grande), and western US (R14: Upper Colorado, R15: Lower Colorado, R16: Great Basin, R17: Pacific Northwest, and R18: California) for presentation and discussion in Section 3.

3. Results

3.1. Model evaluation

To evaluate RegCM4-simulated baseline runoff against the control-run runoff, we compare the cumulative probability distribution of simulated monthly average runoff during the overlapping historical period (1981–2005) in Fig. 4. For reference, observed runoff from the WaterWatch dataset is also shown for the same period. Although, the magnitude of the monthly average runoff mostly compares well between control-run simulation and the WaterWatch-based runoff, a few regions show biases in the control-run VIC simulations when compared with observation. For instance, large differences can be seen in Region 1 where the VIC model underpredicted the monthly runoff. Similarly, Region 4 also shows dry bias above 80th percentile, whereas Region 11 and 12 show a wet bias above 60th percentile relative to observation. Additionally, major disagreements also exist between control-run and RegCM4-simulated monthly runoff, including a wet bias in the eastern regions (Regions 1, 2, and 3) (Fig. 4a–c) and a dry bias in the Midwest (i.e., Regions 4, 5, 7, and 9) and Southwest (i.e., Regions 13, 14, 15, and 16). Note that our RegCM4 bias correction is conducted using the 1966–2005 climatology. Therefore, while the monthly distributions of mean temperature and precipitation between 1966 and 2005 observation and baseline simulation are identical, there could be differences in the 1981–2005 sub-period as a result of different climate interannual variability depicted by each GCM ensemble. In addition to the different climate interannual variability, these runoff biases could also be a result of the residual errors in the magnitudes of RegCM4-simulated daily precipitation and temperature that are not sufficiently corrected by the bias correction. This means that the ten RegCM4 ensembles are not identical after the bias correction, although they have the same mean climatology during the 1966–2005 baseline period.

To further evaluate the performance of runoff extremes simulated by the VIC model, we compare the spatial cumulative probability distributions (across all HUC8s) of the 95th percentile daily runoff value (R95) for each HUC8 and the 30-day moving average 5th percentile runoff value (R5) for each HUC8 throughout CONUS in Fig. 5a and 5b. In general, both the 1981–2005 baseline simulation and control run show very similar results. However, for both R95 and R5, the control run is slightly lower than baseline simulations in wetter HUC8s (cumulative non-exceedance probability greater than 0.7) and slightly higher in drier HUC8s (cumulative non-exceedance probability less than 0.7). To compare the simulated extremes to WaterWatch, we repeat the analysis using monthly runoff and illustrate monthly R95 in Fig. 5c and monthly R5 in 5d. Although the WaterWatch R95 is consistently higher than both control and baseline simulations, the difference between observation and simulation is very small. A much larger difference is revealed for R5, where the VIC simulated monthly R5 are over-predicted by 2–4 mm in around 70% of the HUC8s. This finding of wet-bias is consistent with Shrestha et al. (2014) who also showed difficulties in reproducing low flow extremes, which they attributed to uncertainties related to model structure, calibration, and errors in observed discharge data. We also acknowledged that using monthly high runoff might be problematic for validation purposes, as it may not capture the daily peak runoff that may occur at shorter timescales. Nevertheless, given the unavailability of daily resolution CONUS runoff observation, such comparison cannot be achieved at the current stage. Further development of daily resolution runoff observation at HUC8 scale will be highly useful. Using monthly R5 may not be an issue to validate the low extremes because the low runoff events may take place over longer timescales.

To validate model performance in terms of cold season processes, we compare RegCM4-simulated April 1st SWE with the control-run and Snow Telemetry (SNOTEL) observed snow course data, described in Mote et al. (2005), in the western US (Fig. 6). Because many of the sites are located above the mean elevation of the VIC grid cell, we use the April 1st SWE in the highest elevation band for each VIC grid cell for comparison. The RegCM4-simulated April 1st SWE ensemble compares well with the control-run April 1st SWE but underestimates the SWE relative to SNOTEL observations, particularly at stations with lower SWE on April 1st. This difference suggests model error toward early snow ablation, which might be associated with biases in model snow parameters (roughness and albedo) or underestimation of total winter precipitation. Although identification of the exact drivers of the model biases is beyond the scope of the current study, some potential causes may stem from the differences in the elevations of the VIC model grid cells and the point-based observations as well as known biases in both Daymet and PRISM precipitation data, particularly in

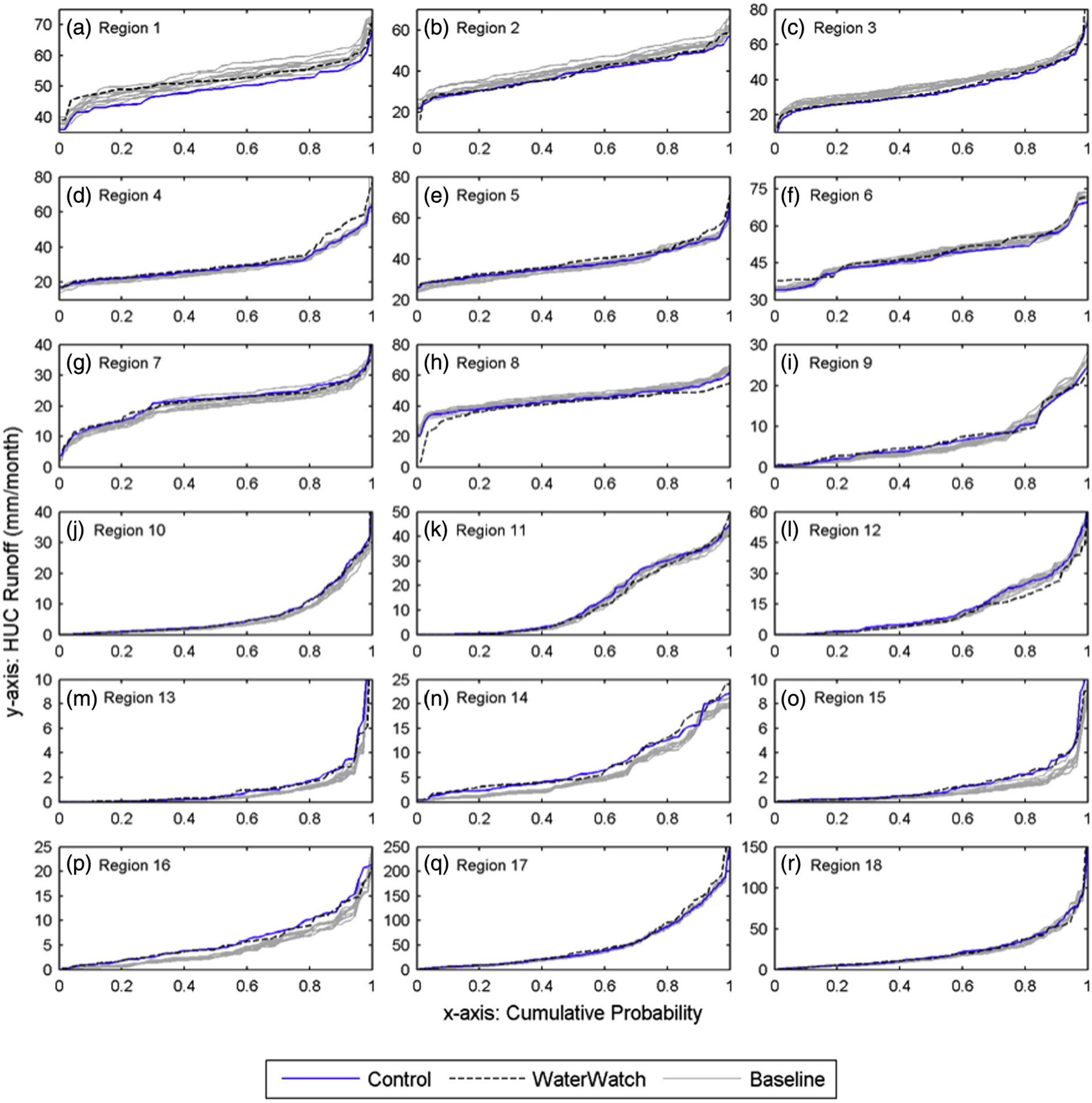

Fig. 4. Cumulative distribution functions of the RegCM4-based simulated mean monthly runoff for the 1981–2005 period compared with control-run simulated and observed monthly runoff.

the high elevation region (e.g., Pan et al., 2003; Sheffield et al., 2003; Tian et al., 2007).

3.2. Regional hydrologic response to climate change

We examine future hydrological response using several types of variables: mean water balance (quantified by P, ET, and R), hydrological extremes (quantified by R95, R5, and time of occurrence of peak runoff events), and cold season processes (quantified by changes in SWE, number of snow-covered days, and winter rain-to-precipitation ratio). For each future simulation, the significance of the median change in total runoff is assessed using the Wilcoxon signed-rank test at the 95% level.

3.2.1. Changes in temperature and precipitation

Fig. 7 shows the projected seasonal multimodel ensemble median change in temperature (°C) and precipitation (%) from the 1966–2005 baseline to the 2011–2050 future periods. A consistent warming from +0.5 to +2 °C is projected across all regions and in all seasons. The greatest temperature rise is projected in summer, particularly in the northern and western US (Fig. 7e). In the northeastern US, the largest increase is projected in winter (Fig. 7a). The projected seasonal changes are generally consistent with the projected seasonal changes in temperature reported by other studies (Hagemann et al., 2013; Liu et al., 2012; Melillo et al., 2014; Kunkel et al., 2010; Ojima et al., 2013).

Compared with temperature, the projected change in ensemble median precipitation has more spatial and seasonal variability. Consistent with previous studies (Rasmussen et al., 2014; Cayan et al., 2013; Seager and Vecchi, 2010; Christensen and Lettenmaier, 2007; Jerla et al., 2012), an increase in winter and spring precipitation (+5 to +13%; Table 2) is projected in the northern and western US (Fig. 7b and 7d), whereas a decrease in winter precipitation is projected in the southwestern US (−3 to −1%). However, summer and autumn precipitation shows little change across many regions (Fig. 7f and 7h), except those in the southern US (i.e., Regions 8, 11, and 12), where an increase in summer precipitation is projected (i.e., about +7%). Similarly, in

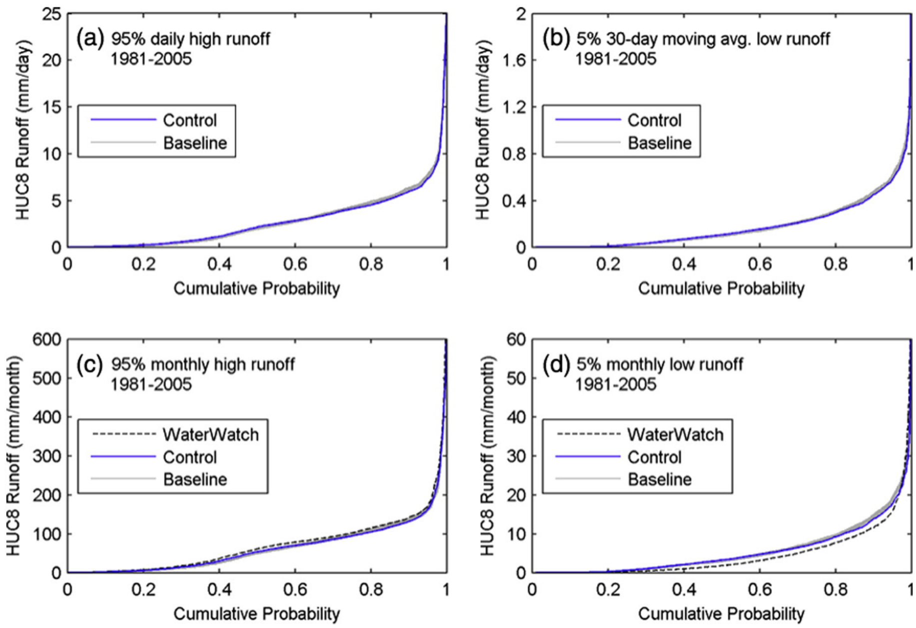

Fig. 5. Comparison of cumulative HUC8 runoff distributions among 1981–2005 RegCM4-based control and baseline simulations and WaterWatch runoff observation for (a) 95% daily high runoff, (b) 5% 30-day moving average runoff, (c) 95% monthly high runoff, and (d) 5% monthly low runoff.

other regions, such as Region 13 (Rio Grande region), a general decrease in annual precipitation was found by most previous studies (Hagemann et al., 2013; Liu et al., 2012; Melillo et al., 2014; Llewellyn and Vaddey, 2013). The winter and spring precipitation projections from the present study also show a slight decrease in this region (i.e., −1 to −4%). In contrast, for the northern regions, most previous studies project a relatively wetter future climate (Kunkel et al., 2013; Reclamation, 2012), consistent with changes in precipitation projected by the present study for the northern regions.

3.2.2. Changes in seasonal runoff

Fig. 8 shows the projected seasonal ensemble median change in total runoff from the 1966–2005 baseline to the 2011–2050 future periods. It also shows the number of GCMs out of ten that project seasonal runoff increase, with dots indicating statistically significant changes detected by at least five or more models in seasonal median runoff for each HUC8. Our results show that most models project increases in winter runoff across all HUC2 regions (Fig. 8a). However, statistically significant change is detected only in the snow-dominated regions (Regions 1, 9, 14, 16, and 17 where, most models project statistically significant increasing changes in winter runoff (Fig. 8b). In contrast, decreases in

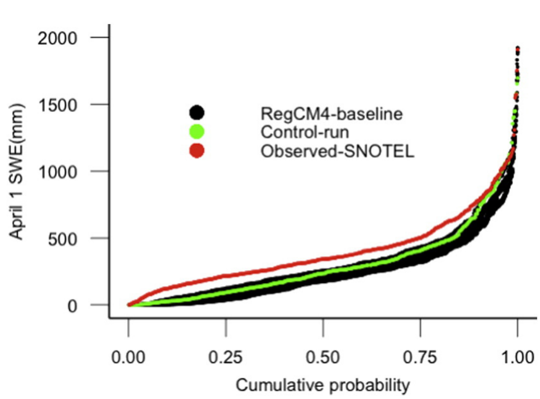

Fig. 6. Cumulative distribution functions of the RegCm4-based simulated mean April 1st snow water equivalent (SWE) for the 1981–2000 period compared with control-run simulated and observed April 1st SWE for the 618 Snow Telemetry (SNOTEL) stations in the western United States.

winter runoff are projected for many subbasins in the southeastern US (i.e., Regions 5, 6, 8, 11, and 12; Fig. 8a). In the southern US, ET is also projected to increase in winter (varying from +0.6% to +6.8%; Table 2) which may also contribute to a decrease in winter runoff and overall winter drying in the southern US. However, these regions have low agreement among the 10 ensemble members (Fig. 8b) and therefore greater uncertainty exists in the direction of change in runoff projections.

As shown in Fig. 8c, an increase in ensemble median spring runoff is also projected across the northern (i.e., Regions 4, 7, 9, and 10) and southern US (Regions 8, 11, 12 and 13). For those regions, the models largely agree on the direction of the change in spring runoff, but statistically significant increases are projected in fewer subbasins, as indicted by blue dots in Fig. 8d. To the west, many regions show spatial variability in runoff projections, ranging from modest increases in spring runoff over Regions 14, 15 and 16 to small decreases in the western portions of Region 17 and in most subbasins of Region 18. These regions also show a projected increase in spring ET (i.e., up to +8.4%) due mainly to the warmer temperatures and excessive soil moisture from increased precipitation and snowmelt. These positive ET changes appear to be primarily driven by increasing temperatures and higher soil moisture contents from increased precipitation and snowmelt in winter and spring. Similarly, in the eastern US (Regions 1 and 2 and portions of Regions 3, 5 and 6) there is a decrease in ensemble median spring runoff (Fig. 8c). However, the uncertainty of the spring runoff projections is greater for the eastern US. Few models agree on the sign of the projected change, except in the Northeast, where there is strong consensus among models in the projected decrease of runoff, particularly in Region 1 and in the northern subbasins of Region 2 (Fig. 8d).

In contrast, runoff projections for the summer are spatially heterogeneous, with notable reductions in ensemble median summer runoff for most of the western HUC8s (−1.8% to −5.2%) and in the Northeast (i.e., up to −12% in Region 1). These regions also show small decreases in summer ET (−4.4% to −1.2%; Table 2), which is potentially associated with a summertime decrease in soil moisture resulting from low summer precipitation and runoff. In contrast to western regions, more pronounced increases of up to 20% in summer runoff is projected over the northern and southern US (Fig. 8e). Note, however, that in most southern regions (i.e., Regions 8, 11, 12, and 13), although projected precipitation increases are modest (+5 to +8%), changes in total runoff are

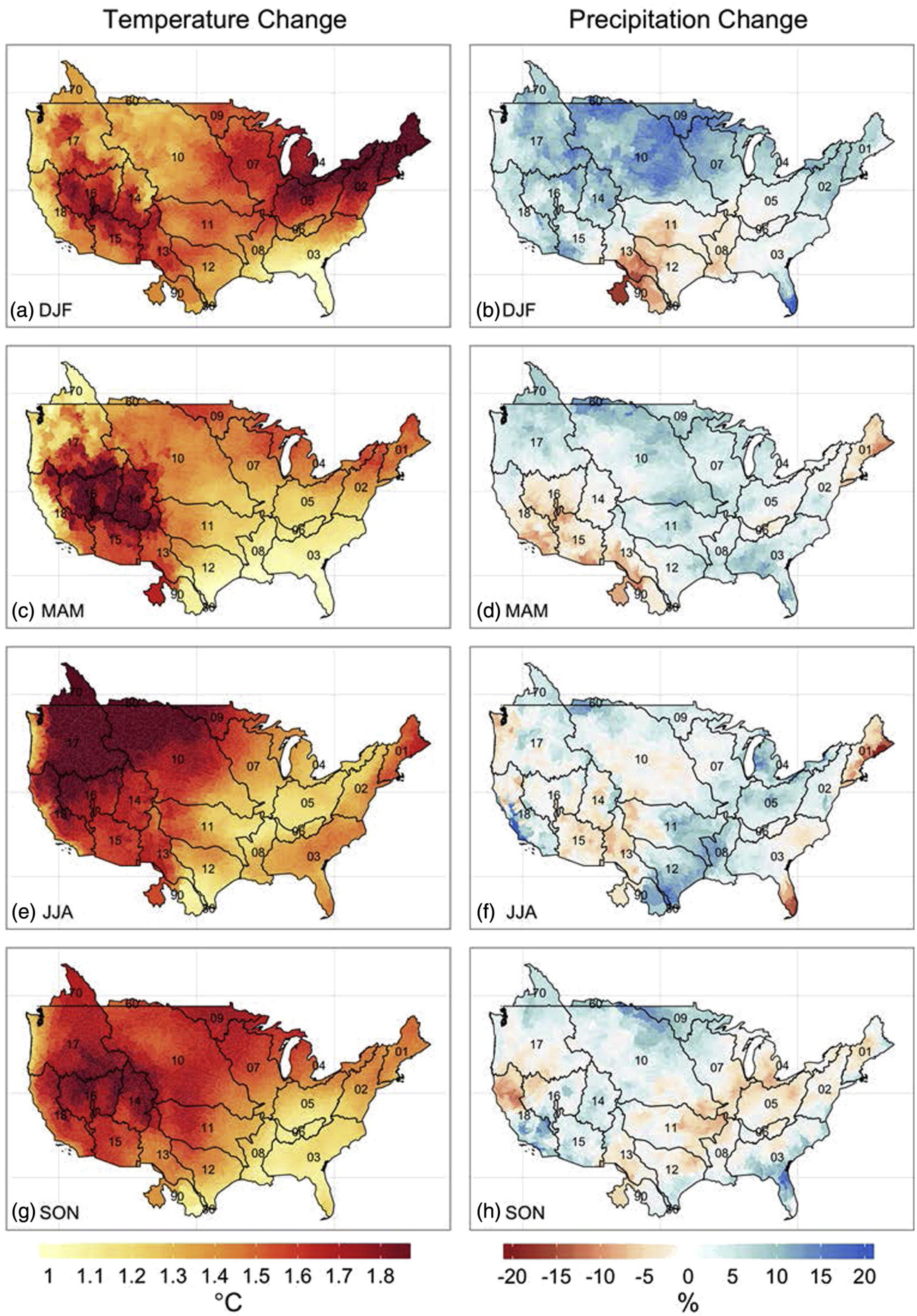

Fig. 7. Ensemble median seasonal percentage changes in temperature for 2011–2050 under the RCP 8.5 emissions scenario relative to 1966–2005 for (a) DJF, (c) MAM, (e) JJA, and (g) SON seasons; and precipitation change for (b) DJF, (d) MAM, (f) JJA, and (h) SON seasons in each 8-digit hydrologic unit code (HUC8) subbasin. (Notes: DJF = December/January/February; MAM = March/April/May; JJA = June/July/August; SON = September/October/November).

larger (+5 to +22%; Table 2). This indicates that small changes in precipitation can enhance the runoff response when accompanied by changes in precipitation intensity and timing. Earlier studies also show that a 10% increase in annual precipitation can lead to increases in runoff of more than +40% (Goudie, 2006; Gordon and Famiglietti, 2004). Despite the spatial variability in summer runoff projections across the US, the signal for summer runoff changes is robust because most of the models agree on the sign of the projected change in most regions (Fig. 8f).

The variations among ensemble median runoff change projections for autumn are relatively similar to variations among summer runoff projections across all HUC2 regions (Fig. 8g). More decreases are

Table 2
Multimodel ensemble median projected seasonal change in precipitation, temperature, evapotranspiration, and total runoff in the near future (2011–2050) relative to the baseline period (1966–2005) summarized by HUC2 and various regions. The models used in the analysis are described in Table 1.

	Temperature (°C)				Precipitation (%)				ET (%)				Total runoff (%)			
	DJF	MAM	JJA	SON	DJF	MAM	JJA	SON	DJF	MAM	JJA	SON	DJF	MAM	JJA	SON
CONUS	1.4	1.5	1.4	1.4	5.11	2.88	2.61	0.09	2.74	3.80	−0.13	2.78	14.13	11.98	9.46	9.99
Eastern US	1.4	1.2	1.3	1.1	3.96	2.55	1.00	1.01	4.38	2.96	−0.99	1.29	7.69	3.64	3.66	5.33
Region 1	1.7	1.4	1.5	1.3	7.69	−4.34	−4.64	−0.79	1.04	6.72	−1.40	−0.62	12.14	−7.51	−12.14	−1.33
Region 2	1.5	1.3	1.3	1.2	8.55	0.88	2.13	−0.70	3.75	3.58	0.55	2.29	11.73	−0.72	−1.47	3.76
Region 3	1.1	1.0	1.4	1.0	1.79	5.52	0.27	4.88	4.81	1.35	−1.85	1.74	5.67	6.57	5.54	7.44
Region 5	1.6	1.2	1.2	1.1	2.78	1.41	5.16	−3.81	4.56	3.58	0.26	2.97	3.08	1.78	8.02	1.13
Region 6	1.3	1.2	1.2	1.0	−0.24	−1.38	1.18	−1.41	9.02	2.72	−0.70	1.74	−0.37	2.17	0.53	1.83
Northern US	1.5	1.4	1.5	1.6	10.44	5.69	3.27	1.95	−1.12	5.52	1.82	5.00	20.06	18.08	13.49	9.39
Region 4	1.7	1.4	1.4	1.4	8.87	4.64	7.04	0.03	−3.79	4.57	2.21	4.80	14.58	5.54	9.69	2.61
Region 7	1.6	1.4	1.4	1.5	10.48	5.11	2.99	1.40	−5.99	3.17	0.39	4.32	12.45	11.68	9.73	5.24
Region 9	1.4	1.5	1.7	1.7	13.29	7.79	3.27	7.79	−1.93	5.01	3.74	8.10	24.61	27.53	22.90	16.71
Region 10	1.3	1.4	1.7	1.6	11.11	5.70	1.30	2.94	1.62	5.66	1.01	4.23	12.99	16.28	8.29	6.16
Southern US	1.4	1.2	1.2	1.3	−3.08	2.56	5.44	−0.91	3.12	0.64	−0.06	2.57	8.05	15.14	21.52	20.88
Region 8	1.2	1.1	1.1	1.1	−3.81	4.59	8.14	−0.76	6.54	1.54	−0.89	2.74	−2.76	8.63	17.17	8.10
Region 11	1.4	1.3	1.3	1.4	−1.11	4.48	5.46	−1.98	4.98	2.10	−0.95	3.14	4.24	11.48	16.50	9.01
Region 12	1.3	1.1	1.2	1.2	−3.39	1.82	8.60	1.52	3.17	0.10	1.19	1.93	5.02	15.68	22.72	22.44
Region 13	1.4	1.4	1.4	1.4	−3.39	−2.42	−1.10	0.77	0.68	−1.67	−1.60	2.41	5.46	7.13	5.05	7.39
Western US	1.4	1.6	1.7	1.6	7.07	0.47	1.05	1.33	5.08	5.27	−1.49	1.93	18.04	10.37	0.68	5.99
Region 14	1.4	1.8	1.6	1.6	6.7	8.24	−0.01	−0.45	0.72	5.63	−1.20	4.43	10.52	19.98	−4.46	0.07
Region 15	1.5	1.6	1.6	1.5	9.6	1.69	−5.48	−2.76	6.64	−1.50	−4.49	2.90	25.58	12.07	9.73	21.23
Region 16	1.5	1.8	1.8	1.7	6.7	5.79	−2.15	0.50	1.62	4.62	−2.52	−0.71	12.32	10.00	−1.82	1.42
Region 17	1.4	1.4	1.8	1.6	5.3	8.53	4.73	0.76	6.07	8.45	1.74	3.69	11.76	5.13	−5.26	−0.31
Region 18	1.3	1.3	1.6	1.5	9.3	5.57	−1.83	3.32	7.15	3.25	−1.97	−1.71	11.31	−0.15	−1.97	−2.00

expected in the western and eastern regions, while increased runoff is projected in the central US according to most models (Fig. 8h). However, the uncertainty in autumn runoff projections is greater in the areas where runoff is projected to decrease or show no change (i.e., the degree of consensus among models on the direction of change is low in many areas), particularly in the eastern US (Fig. 8h).

3.2.3. Changes in high and low runoff

Fig. 9 shows spatial variations in percentage change in ensemble median R95 and R5 (i.e., high and low runoff, respectively) projections and the degree of consensus among models. In many eastern regions (i.e., Regions 2, 3, 5, and 6), R95 increases only by +5% by the end of 2050, whereas in Region 1, it is projected to decrease by −10%. However, the eastern US, Regions 5 and 6 in particular, exhibits higher uncertainty, as the degree of consensus among models is low (i.e., only half of the models project increases) (Fig. 9b). On the other hand, in regions across the central US (e.g., Regions 9, 10, 11 and 12), there is a strong consensus among models on projected increase in R95 (i.e., up to +20%), whereas Regions 7 and 4 in the northern US show modest increases in high runoff of up to +10% with moderate consensus among models. Over the western US, change in the projected R95 is more variable with areas showing both small increases and decreases in high runoff conditions (Fig. 9a). For example, areas to the east of Regions 17 and 14 and to the north of Region 18 show decreases while some areas in Regions 15, 13 and 14 show increases in R95. However, the change in R95 projections over western US is less certain because models don not exhibit a consensus on the sign of projected changes in many areas (Fig. 9b).

Multimodel ensemble median R5 is projected to decrease in most of the HUC8 subbasins in all eastern regions (on average −1% in Region 5 to −18% in Region 1) and in many western coastal subbasins of Regions 17 and 18 (Fig. 9c). However, increases in R5 runoff of up to +20% are projected in the central US, most notably in Regions 9, 10 and 7. For R5 projections, no clear consensus on the sign of the projected change is, however, evident in much of the US (Fig. 9d), except in Regions 9 and 10 where moderate consensus is found on positive R5 change and in Regions 1 and 17, where most models give negative change in low runoff conditions. The general tendency toward an increase in the magnitude of high runoff but decrease in low runoff in the future period suggests the possibility of more wet and dry extremes. It should be noted that the largest signal of low runoff decreases occurs in Regions 1 and 17 where summer precipitation is also projected to decrease (Fig. 7f).

3.2.4. Changes in snow and occurrence of maximum peak runoff

An analysis of future changes in the cold season processes is shown in Fig. 10. For the eastern US, our results indicate a decrease in April 1st SWE (−50%), snow-covered days (−25 days/year), and annual maximum SWE (−20%) across many eastern regions (Fig. 10b-c) that presently receive a part of their precipitation as snow during winter months. Fig. 10d also shows increases in the cold-season (November to March) rain-to-precipitation ratio. This is likely to be a result of warmer winter temperatures (Fig. 7a) that may cause more precipitation to fall as rain rather than snow. Similarly, in the eastern US, a shift in the runoff peak to earlier in the spring as well as a higher probability of occurrence of peak annual runoff in autumn and winter (Julian days 270–330) are projected (Fig. 11a). However, we note that the inter-ensemble variability is larger in these regions.

In the northern US, a mix of increases in winter and spring precipitation and warmer temperatures leads to the heterogeneous snow hydrology response. For instance, the annual maximum SWE and number of snow-covered days are projected to decrease (by −10% and −20 day/year, respectively) in Regions 4 and 7 (Great Lakes and Upper Mississippi regions, Fig. 10b and c). On the other hand, in Regions 9 and 10 (the Souris-Red-Rainy and Missouri), the annual maximum SWE is expected to increase (Fig. 10b) without any change in snow-covered days (Fig. 10c). Our results also show small changes in the winter rain-to-precipitation ratio (±0.01) in the northern US (Fig. 10d) despite the increase in winter temperatures (Fig. 7e) as, even with warming, temperatures still remain below freezing. The muted rain-to-precipitation response in Regions 9 and 10 leads to no future changes in the timing of peak runoff (Fig. 11b). However, exceptions exist in Region 4 and in some parts of Regions 7 and 10, where the rain-to-precipitation ratio shows an increase of +0.04 to +0.1, consistent with a general decrease in snow in those areas. These regions also show decreased probability of occurrence of peak annual runoff in the spring (Julian days 50–100) and increased probability in the summer (Julian days 150–200) (Fig. 11b). In the northern US (i.e., Regions 4, 5 and 7), where maximum

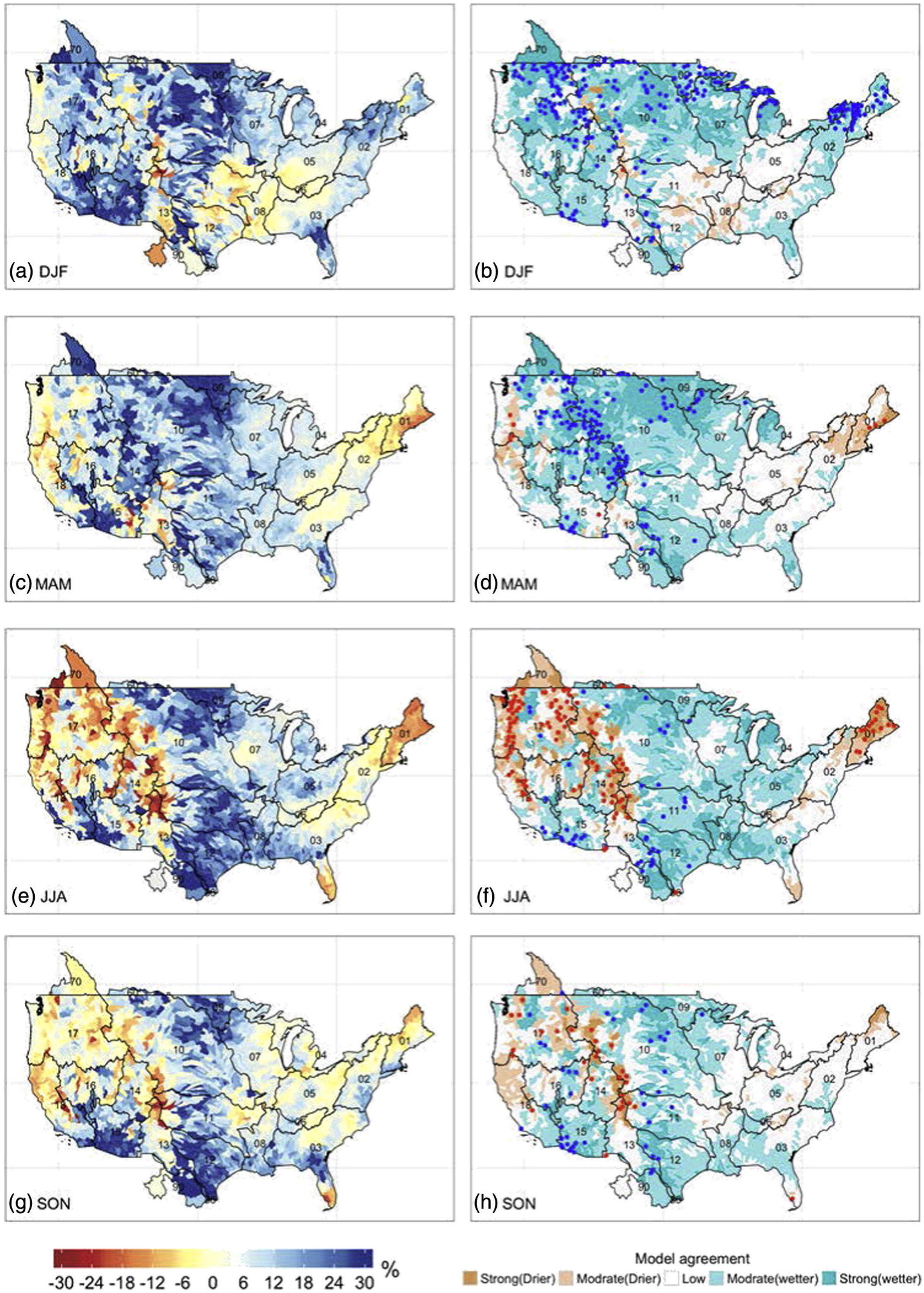

Fig. 8. Ensemble median seasonal percentage changes in total runoff for 2011–2050 under the RCP 8.5 emissions scenario relative to 1966–2005 for (a) DJF, (c) MAM, (e) JJA, and (g) SON seasons; and number of ensemble of members out of 10 CMIP5 models that project a total runoff increase in each HUC8 subbasin for (b) DJF, (d) MAM, (f) JJA, and (h) SON seasons. Dots indicate statistically significant change (Wilcoxon signed-rank test at the 95% level) in median seasonal runoff projected by at least half of the models for each HUC8 basin. The numbers refer to the HUC2 identification of hydrologic regions as shown in Fig. 2. (Notes: DJF = December/January/February; MAM = March/April/May; JJA = June/July/August; SON = September/October/November.)

flow occurs in early spring when frozen ground begins to thaw, decreased probability in spring runoff may be associated with changes in freeze/thaw cycles due to projected warmer temperature combined with increases in winter rainfall, as shown in Fig. 10d. Similarly, the increased probability in the occurrence of peak annual runoff occurrence in the summer is more likely due to the projected increase in summer precipitation intensity in these regions.

In the southern US, a decrease of −20% in annual maximum SWE is projected (Fig. 10b). This change is potentially due to the decrease in winter precipitation (Fig. 7e). Also, a small decrease in the number of

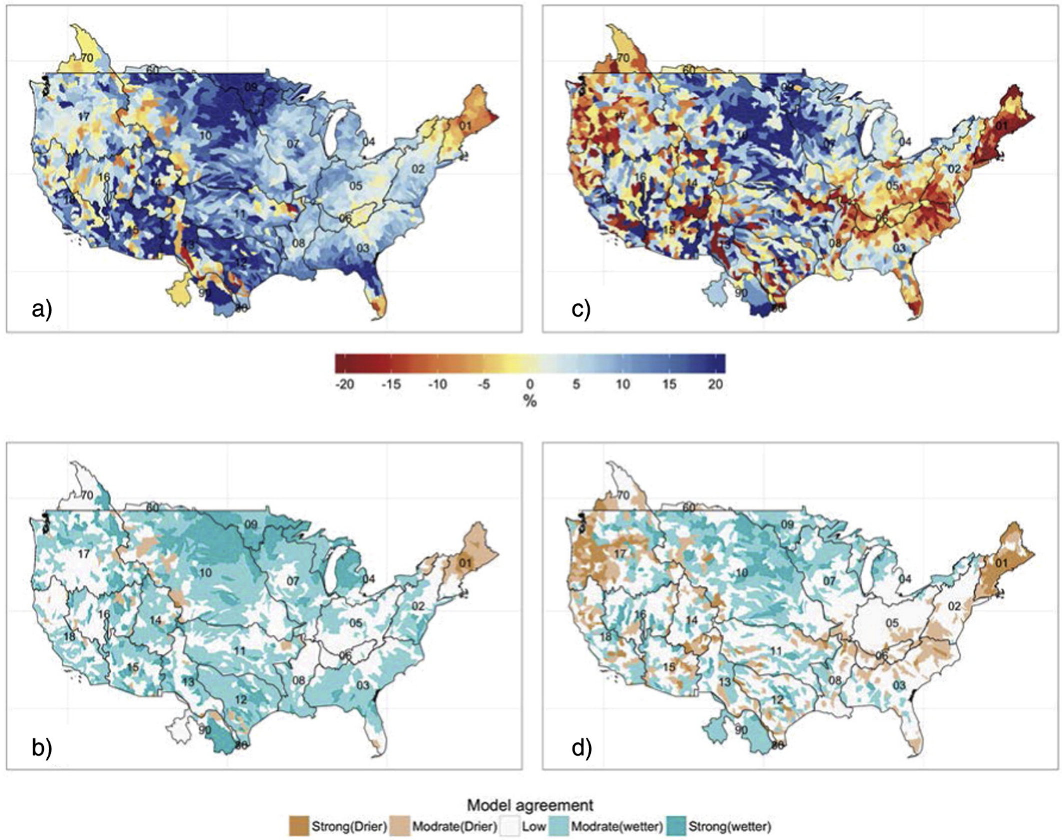

Fig. 9. Ensemble median percentage changes in (a) high runoff (the 95th percentile of daily runoff) and (b) low runoff (7-day low runoff), (c) number of models that predict increase in high runoff and (d) number of models that predict an increase in 7-day low runoff. The numbers refer to the HUC2 identification of hydrologic regions as shown in Fig. 2.

snow-covered days and rain-to-precipitation ratio (~0.02) is projected (Fig. 10d), because the amount of precipitation that falls as snow in these rainfall-dominated regions is relatively low and the change in the fraction of rainfall is largely unaffected. Moreover, the probability of occurrence of peak runoff is also projected to increase in the spring and summer seasons, particularly in Regions 8 and 11 (Fig. 11c); the increase is primarily associated with runoff increases in spring and summer and annual high runoff (Figs. 8c–e and 9a). Additionally, the probability of autumn and winter peak runoff is likely to decrease, particularly in Regions 8, 11 and 12 (the Lower Mississippi, Arkansas and

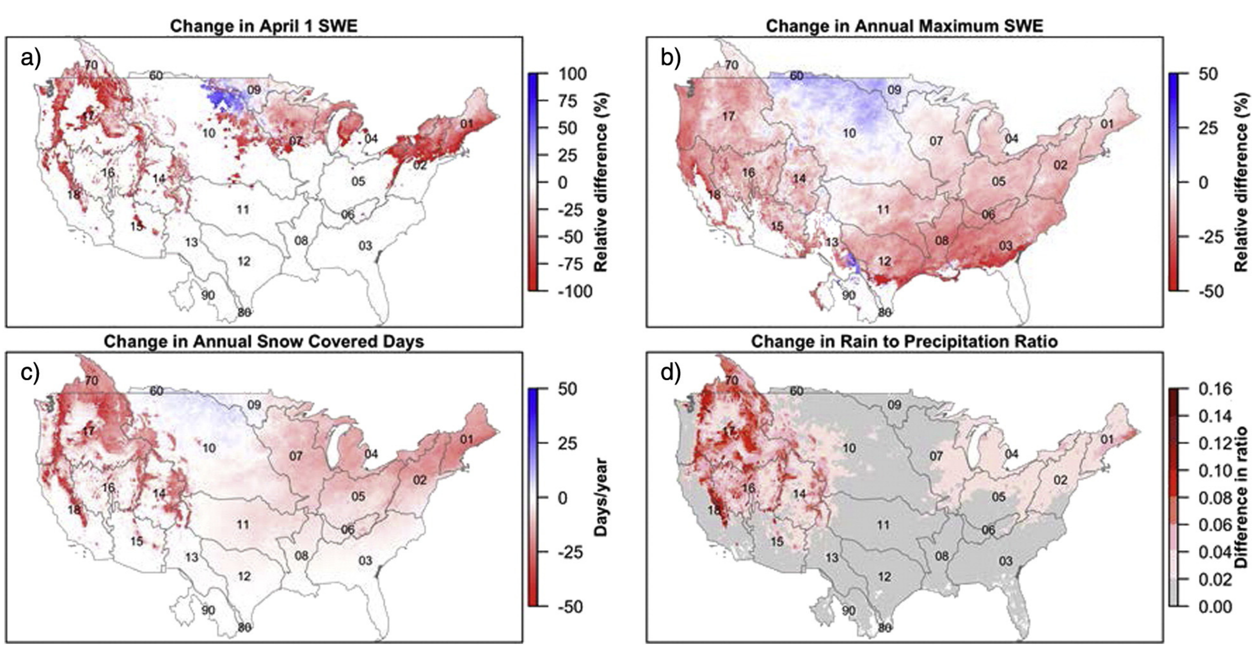

Fig. 10. Ensemble median change (future minus baseline) in the (a) April 1st snow water equivalent (SWE), (b) annual maximum SWE, (c) annual snow-covered days, and (d) change in the rain-to-precipitation ratio.

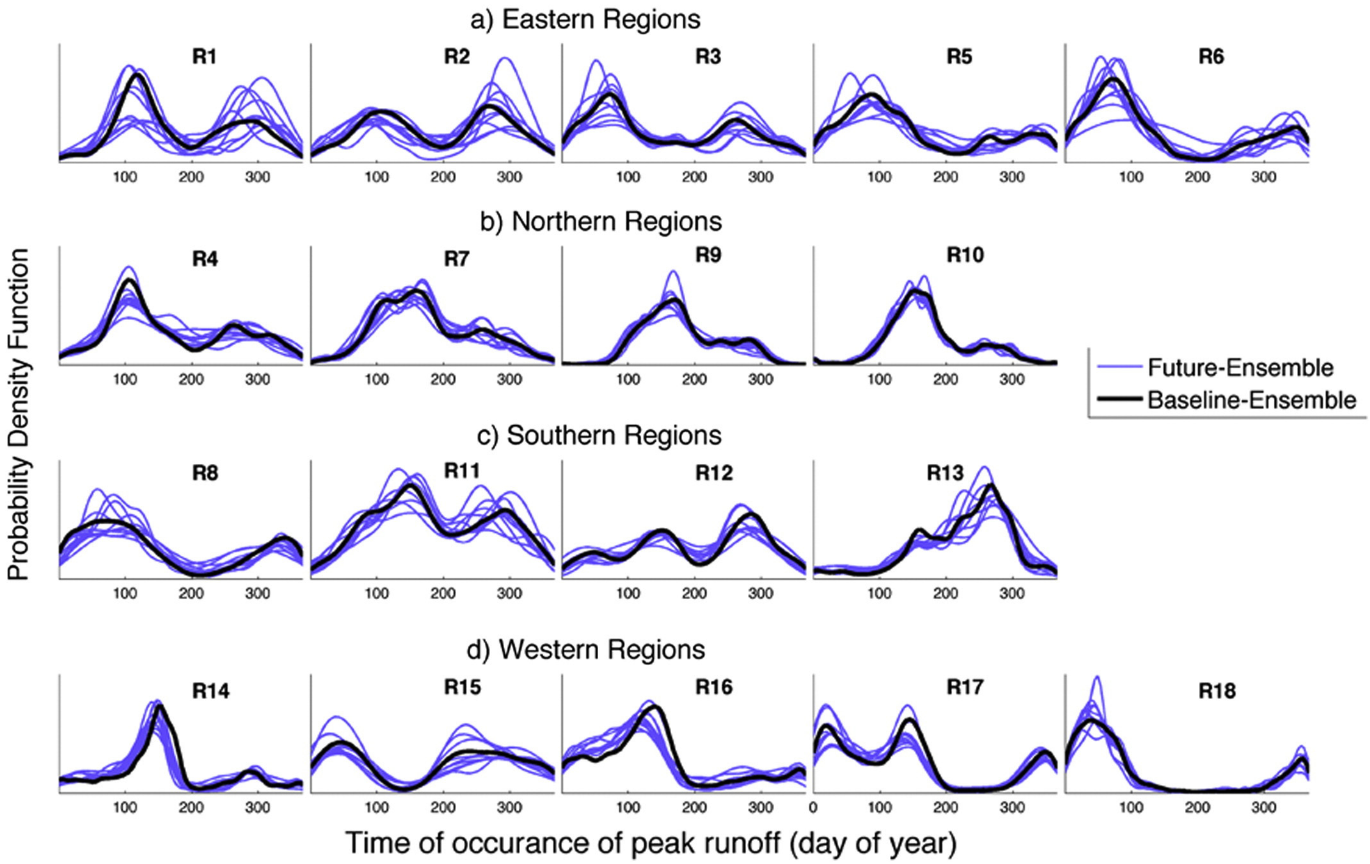

Fig. 11. Probability density function (PDF) of time occurrence of annual peak runoff in the near future period (2011–2050) for each HUC2 region: (a) eastern, (b) northern, (c) southern, and (d) western. PDFs are presented for all climate model projections as listed in Table 1. The solid black line is the multimodel ensemble of time occurrence of peak runoff for the baseline period.

Texas; Fig. 11c), a change primarily associated with the decrease (increase) in winter precipitation (ET) in these regions (Fig. 7a and Table 2).

Similarly, changes in the snow hydrology in the western US suggests a widespread decrease of more than −50% in April 1st SWE (Fig. 10a) and a reduction of −25 days/year in the snow-

Table 3
Summary of hydrologic responses projected in the near future (2011–2050) relative to the baseline period (1966–2005) summarized by HUC2 regions and comparison with previous studies. The highlighted studies indicate that these studies do not agree with the direction of projected change in present study.

	Projected hydrologic response (this study)	HUC2 regions*	Projected hydrologic response (other studies)
Eastern US	Increase in winter runoff	1,2,3,5	Hayhoe et al. (2007); Stagge and Moglen (2013); Pradhanang et al. (2013)
	Decrease in summer runoff	1,2	Huntington et al. (2009); Hayhoe et al. (2007); Stagge and Moglen (2013); Bastola (2013); Pradhanang et al. (2013)
	Increases in high runoff	2,3,5,6	Stagge and Moglen (2013)
	Decreases in low runoff	1,2,5,6,3	Frumhoff et al. (2007); Hayhoe et al. (2007); Stagge and Moglen (2013)
	Decrease in April 1st SWE, maximum SWE and snow-covered days	1,2,3,5,6	Hayhoe et al. (2007); Pradhanang et al. (2013); Matonse et al. (2011)
	Earlier shift in peak runoff	1,2	Frumhoff et al. (2007); Hayhoe et al. (2007)
Northern US	Increase in winter, spring runoff	4,7,9,10	Cherkauer and Sinha (2010); Chien et al. (2013)
	Increase in summer runoff	4,7,9,10	Chien et al. (2013); Cherkauer and Sinha (2010)
	Decrease in autumn runoff	4,7	Cherkauer and Sinha (2010)
	Increases in high and low runoff	4,9,10	
	Decrease in April 1st SWE, maximum SWE and snow-covered days	4,7	Notaro et al. (2014)
	Increase in annual maximum SWE	9,10	Sinha and Cherkauer (2010)
Southern US	Decrease in winter runoff	8,11,12	
	Increases in spring, summer and autumn runoff	8,11,12,13	Seager et al. (2013); Milly et al. (2005)
	Increases in high and low runoff	8,11,12	
Western US	Increase in winter runoff	14,15,16,17,18	Rasmussen et al. (2014); Maurer (2007); Vano et al. (2014); Maurer and Duffy (2005)
	Decrease in summer and autumn runoff	14,16,17,18	Ficklin et al. (2013); Rasmussen et al. (2014); Hamlet et al. (2013); Maurer and Duffy (2005)
	Increases in high runoff	14,15,16	
	Decreases in low runoff	17,18	Tohver et al. (2014)
	Decrease in April 1st SWE, maximum SWE and snow-covered days	14,15,16,17,18	Garfin et al. (2014); Maurer (2007); Mote et al. (2003); Klos et al. (2014); Ashfaq et al. (2013); Mankin and Diffenbaugh (2014)
	Earlier shift in peak runoff	14,16,17	Hamlet et al. (2013); Maurer (2007); Stewart et al. (2004); Hidalgo et al. (2009)

* HUC2 regions identified by the direction of change in median multimodel ensemble projections.

covered period (Fig. 10c). The reduction in snow-covered days, despite the increase in winter precipitation, suggests more dependence on temperature changes (Fig. 7a–d) through an increase in the frequency of freeze-thaw cycles and the likelihood of accelerated melt rates. This temperature dependence is substantiated by an increase in the rain-to-precipitation ratio in cold-season months (Fig. 10d). This is further supported by Fig. 11d, which shows increases in the probability of annual peak runoff and a shift in its timing to the early spring/winter season. These shifts in hydrological timing are more evident in Regions 14, 16 and 17 (Fig. 11d). Our results indicate that the peak in spring runoff will shift to 5 to 10 days/year earlier by the end of the mid-21st century in these regions. Such a shift in the runoff regime, combined with increases in winter rainfall, suggests that more water is available for runoff earlier in the spring (Fig. 11d), which may contribute to drier conditions in the summer but could also increase the risk of winter and spring floods.

4. Discussion

Our analysis of potential impacts of climate change on hydrological response in the CONUS, as summarized in Table 3, shows that there is a spatial and temporal heterogeneity in the runoff response resulting from a combination of changes in temperature and precipitation as discussed below.

4.1. Changes in seasonal runoff response

Our results show a general agreement with previous climate change impact studies regarding the types and direction of future projected changes across different regions of the CONUS (Table 3). In this study, most hydrologic simulations suggest increases in winter runoff in northern and eastern regions and across the western US, consistent with other studies (e.g., Vano et al., 2014; Karl et al., 2009; Frumhoff et al., 2007; Hayhoe et al., 2007). Unlike the increases in winter runoff, the summer runoff change is projected to decreases in the Northeast (e.g., in Region 1 and 2) and most regions of western US. Such changes and shifts in the runoff regime indicate that simultaneous increases in temperature and precipitation will lead to wet springs and dry summers and impact the distribution of water availability during the water year, particularly in the snow-dominated regions. Hamlet et al. (2013) also showed shifts in streamflow timing from spring and summer to winter in the Pacific Northwest associated with decreases in spring snowpack in basins with significant snow accumulation in winter, generally consistent with the snow projections described in Section 3.2.4.

In contrast to HUC2 regions in the western and eastern US, our results show that spring and summer total runoff will increase in the northern and southern US (Figs. 8c and 7e). However, the causes related to changes in runoff likely vary greatly from region to region. In the northern US, these positive changes appear to be primarily driven by increasing temperatures and increased summer precipitation (Fig. 7e and 7f) and a projected increase in high runoff conditions (Fig. 9a). Cherkauer and Sinha (2010) also found projected increases in summer peak flows and mean flows in the Great Lake regions by end of this century, which they associated with increased occurrence and magnitude of summer storm events. The increase in summer runoff, however, did not agree with Chien et al. (2013) who showed decreased summer flow in the Midwestern US. They used an ensemble of nine GCMs applied across three emissions scenarios (A2, A1B, and *B*1) to quantify potential climate change impacts on streamflow for 2046–2065 and 2081–2100 and attributed the reduction in summer flow to combined effects of decreased precipitation and increased ET due to projected warmer temperatures.

On the other hand, in the southern US, the increase in summer runoff might be attributable to more intense precipitation events associated with mesoscale convective complexes (Ashley et al., 2003) that may produce a larger fraction of runoff because of an increase in infiltration-limited runoff associated with greater intensity. The increases in summer runoff in the southern US, however, are in contrast to declining summer runoff trends shown by previous studies (Seager et al., 2013; Milly et al., 2005) in this region. These differences with earlier studies may be due to the different driving GCMs, and also in part to their use of GCM data that were not dynamically downscaled and struggle to represent warm season convective precipitation extremes over the southern plains (Harding et al., 2013). Anderson et al. (2003) also show that RCMs capture such mesoscale events more accurately than global models do. It should be noted that these contrasting results with other available studies might also be due to several other factors, such as differences in spatial domain, differences in GHG emissions scenarios in the models and the different spans of the baseline and projection periods.

4.2. Changes in high and low runoff

Consistent with total runoff changes, climate change is also likely to affect the frequency and magnitude of high and low runoff events. Our results show a general increase in R95 (high runoff) magnitude across all regions, with a more pronounced increase projected in the northern and southern regions (Fig. 9a; Table 3). However, the projected change in R95 is more variable across the eastern and western US, ranging from moderate increases in many basins to slight decreases in some parts of Region 10 (i.e., along the Rocky Mountains) and in Region 1. The decreases in high runoff in the snow-dominated basins might be related to the slow shift from a snow-melt dominated peak flow regime to a summer convective storm dominated peak flow regime, which may result in a short term decrease in peak flows, followed by an increase later in the century.

These changes in high runoff agree with the direction of change that has already been observed or projected for the future. For instance, the increases in high runoff in the central US are consistent with increasing flood trends over the Missouri River basin (Mallakpour and Villarini, 2015) and projected increases in heavy precipitation over Regions 4, 5 and 7 (Wuebbles and Hayhoe, 2004). Similarly, the spatially variable response in high runoff over the western US is also consistent with other studies (Tohver et al., 2014; Chang and Jung, 2010; Mote et al., 2003; Loukas et al., 2002), which show that many areas in the Pacific Northwest region are not experiencing an increase in flood risk but are more likely to have a severe low flow risk. Our results also confirm that R5 (low runoff) is projected to decrease more prominently along coastal basins in the western and eastern US. These future changes in extreme runoff conditions indicate the possibility of increasing flood risks in winter and spring and drought risks in summer.

4.3. Uncertainty in hydrologic projections

Our results also suggest that the degree of uncertainty in projecting future hydrologic response is dependent on seasonal and spatial variability in runoff projections. Projections of winter runoff are more reliable because most of our ensemble members agree on the direction of runoff change in many regions; but they are less certain over southern regions, where a moderate decrease in winter runoff is projected (see Fig. 8a). Similarly, over the eastern US, a decrease in spring runoff is less certain because projections from different models diverge; but they are more reliable in the areas where increases in spring runoff are projected. In contrast, the signal for summer runoff change is robust because there is a strong consensus among the ensemble members on the sign of the projected change, whereas they show higher uncertainly regarding autumn runoff for most regions. The degree of uncertainty in extreme hydrologic projections is also spatially variable, with relatively higher uncertainty regarding low runoff change in many subbasins of the eastern and western regions (shown in Fig. 9d). However, for high runoff, a majority of ensemble members agree on the direction of change over most of the US (shown in Fig. 9b). Uncertainty in hydrological extremes may also be inherent from discrepancies between the RegCM4 ensembles and control-run simulated hydrological extremes relative to observation, especially given that the VIC model calibration is performed using monthly runoff data. For instance, in this study, the discrepancies in reproducing the low flows using the control run and downscaled-RegCM4 data (Fig. 5d) may also contribute to higher uncertainties in the low flow signal. Additionally, some uncertainties in the extremes may also remain due to the fact that statistical bias-correction, as used in this study, performs downscaling at monthly time scale and then disaggregates into daily time step.

5. Conclusions

This study presents the results of simulated regional hydrologic responses to projected climate changes in the CONUS. We use a high-resolution hydrologic model to project changes in key hydrologic indicators, forced by high-resolution climate forcings from a ten-member dynamical downscaled ensemble of CMIP5 GCMs through an RCM under RCP 8.5 with further statistical bias correction. The analysis in this study enables us to understand how future changes in daily temperature and precipitation distributions, will impact runoff characteristics as well as changes in extreme hydrological events at regional and local scales. The following conclusions can be drawn from our analysis:

1. Multimodel median temperature in the CONUS is projected to increase between +0.5 to +2.0 °C by the mid-21st century relative to the baseline period of 1966–2005. For most of the northern and western US, the projected increases in summer temperatures are larger than the increases in other seasons.
2. Precipitation is projected to increase by up to +20% in the winter in much of the US, whereas summer precipitation may remain constant or may decrease slightly, with decreases primarily in the southwestern US.
3. Important signals of seasonal runoff changes include: (a) Increases in winter and spring runoff and decreases in summer runoff, which are more evident in the western and eastern US. These changes appear to be caused by increasing snowmelt (due to warmer temperatures) during winter and spring. (b) Although very little change in precipitation is projected in southern areas, the projected percentage increase in total runoff is large. This indicates that small changes in precipitation can be enhanced into strong runoff response. (3) In northern regions (i.e., Regions 9 and 10), most of the seasonal changes in runoff are expected to increase, driven largely by year-around increases in precipitation.
4. High and low runoff (i.e., 95th and 5th percentile) conditions are likely to increase, particularly in the central and southwestern US, while a projected reduction in low runoff conditions is more pronounced in the western and eastern US.
5. The decrease in April 1st SWE and annual maximum SWE is projected to be greater than 20% across all regions. A decrease in snow-covered days is also projected across all regions, except Regions 9 and 10.
6. Consistent with the projected changes in snowpack and increase in the cold-season rain-to-precipitation ratio (Fig. 10d), the time of occurrence of peak runoff suggests an increasing probability of projected annual peak runoff occurrences in the early spring or the late winter seasons in the snow-dominated regions of the western and eastern US (Fig. 11a, 11d).
7. Our results show that uncertainty in future hydrologic projections is variable over space and time. The uncertainty is higher in projecting future spring and fall runoff changes than winter and summer runoff changes. Similarly, seasonal runoff changes are relatively less certain in eastern US regions than in the northern and western US regions.

This study provides a more comprehensive and detailed understanding of the direction and the magnitude of projected hydrologic response to climate change at regional and subbasin scales for the entire CONUS. Some uncertainties remain, related to the choice of GCMs or hydrologic models that may not capture all relevant physical catchment characteristics, and associated processes such as water management regulations or potential feedback between land cover change and climate change, or vegetation water use in a changing climate. Similarly, it is well known that dynamical downscaled projections are sensitive to the choice of the RCM (e.g., Ayar et al., 2015) particularly in the simulation of warm season precipitation and convectively driven regional-scale circulations. Therefore, despite the use of a large number of driving GCMs, use of a single RCM in our modeling setup is incapable to capture the uncertainty associated with RCM internal biases and convective parameterizations (e.g., Christensen et al., 2001; Alexandru et al., 2007; Giorgi and Gutowski, 2015). Despite these limitations, the projected hydrological changes described in this study will have important implications for many aspects of water resources, including agricultural water supply, flooding and drought conditions, water quality, and reservoir design and operation.

Acknowledgments

We thank the editor and anonymous reviewers for their insightful and constructive comments. This study was funded by the Regional and Global Modeling Program, Office of Science, and the Wind and Water Power Technologies Office, Office of Energy Efficiency and Renewable Energy of the US Department of Energy (DOE), and supported a DOE Report to Congress under Section 9505 of the SECURE Water Act of 2009 (Public Law 111-11). This research used resources of the Oak Ridge Leadership Computing Facility at the Oak Ridge National Laboratory (ORNL). The ORNL authors are employees of UT-Battelle, LLC, under contract DE-AC05-00OR22725 with DOE. Accordingly, the US Government retains and the publisher, by accepting the article for publication, acknowledges that the US Government retains a non-exclusive, paid-up, irrevocable, world-wide license to publish or reproduce the published form of this manuscript, or allow others to do so, for US Government purposes. The US DOE will provide public access to these results of federally sponsored research in accordance with the DOE Public Access Plan (http://energy.gov/downloads/doe-public-access-plan).

References

Abatzoglou, J.T., 2011. Influence of the PNA on declining mountain snowpack in the Western United States. Int. J. Climatol. 31 (8), 1135–1142. http://dx.doi.org/10.1002/joc.2137.

Abatzoglou, J.T., Brown, T.J., 2012. A comparison of statistical downscaling methods suited for wildfire applications. Int. J. Climatol. 32 (5), 772–780. http://dx.doi.org/10.1002/joc.2312.

Ahmed, K.F., Wang, G., Silander, J., Wilson, A.M., Allen, J.M., Horton, R., Anyah, R., 2013. Statistical downscaling and bias correction of climate model outputs for climate change impact assessment in the US northeast. Glob. Planet. Chang. 100, 320–332. http://dx.doi.org/10.1016/j.gloplacha.2012.11.003.

Alexandru, A., de Elia, R., Laprise, R., 2007. Internal variability in regional climate downscaling at the seasonal scale. Mon. Weather Rev. 135, 3221–3228. http://dx.doi.org/10.1175/MWR3456.1.

Anderson, C.J., Arritt, R.W., Pan, Z., Takle, E.S., Gutowski Jr., W.J., Otieno, F.O., da Silva, R., Caya, D., Christensen, J.H., Lüthi, D., Gaertner, M.A., Gallardo, C., Giorgi, F., Laprise, R., Hong, S.-Y., Jones, C., Juang, H.-M.H., Katzfey, J.J., McGregor, J.L., Lapenta, W.M., Larson, J.W., Taylor, J.A., Liston, G.E., Pielke Sr., R.A., Roads, J.O., 2003. Hydrological processes in regional climate model simulations of the central United States flood of June–July 1993. J. Hydrometeorol. 4 (3), 584–598. http://dx.doi.org/10.1175/1525-7541(2003)004<0584:HPIRCM>2.0.CO;2.

Ashfaq, M., Bowling, L.C., Cherkauer, K., Pal, J.S., Diffenbaugh, N.S., 2010. Influence of climate model biases and daily-scale temperature and precipitation events on hydrological impacts assessment: a case study of the United States. J. Geophys. Res. 115, D14116. http://dx.doi.org/10.1029/2009JD012965.

Ashfaq, M., Ghosh, S., Kao, S.-C., Bowling, L.C., Mote, P., Touma, D., Rauscher, S.A., Diffenbaugh, N.S., 2013. Near-term acceleration of hydroclimatic change in the western US. J. Geophys. Res. 118, 10,676–10,693. http://dx.doi.org/10.1002/jgrd.50816.

Ashley, W.S., Mote, T.L., Dixon, P.G., Trotter, S.L., Powell, E.J., Durkee, J.D., Grundstein, A.J., 2003. Distribution of mesoscale convective complex rainfall in the United States.

Mon. Weather Rev. 131 (12), 3003–3017. http://dx.doi.org/10.1175/1520-0493(2003)131<3003:DOMCCR>2.0.CO;2.

Ayar, P.V., Vrac, M., Bastin, S., Carreau, J., Déqué, M., Gallardo, C., 2015. Intercomparison of statistical and dynamical downscaling models under the EURO- and MED-CORDEX initiative framework: present climate evaluations. Clim. Dyn. 46 (3), 1301–1329. http://dx.doi.org/10.1007/s00382-015-2647-5.

Barnett, T., Malone, R., Pennell, W., Stammer, D., Semtner, B., Washington, W., 2004. The effects of climate change on water resources in the west: introduction and overview. Clim. Chang. 62 (1–3), 1–11. http://dx.doi.org/10.1023/B:CLIM.0000013695.21726.b8.

Bastola, S., 2013. Hydrologic impacts of future climate change on Southeast US watersheds. Reg. Environ. Chang. 13 (1), 131–139. http://dx.doi.org/10.1007/s10113-013-0454-2.

Beigi, E., Tsai, F.T.-C., 2014. GIS-based water budget framework for high-resolution groundwater recharge estimation of large-scale humid regions. J. Hydrol. Eng. 19 (8), 05014004. http://dx.doi.org/10.1061/(ASCE)HE.1943-5584.0000993.

Brakebill, J.W., Wolock, D.M., Terziotti, S.E., 2011. Digital hydrologic networks supporting applications related to spatially referenced regression modeling. J. Am. Water Resour. Assoc. 47 (5), 916–932. http://dx.doi.org/10.1111/j.1752-1688.2011.00578.x.

Brekke, L., Wood, A., Pruitt, T., 2013. Downscaled CMIP3 and CMIP5 Hydrology Projections: Release of Hydrology Projections, Comparison with Preceding Information, and Summary of User Needs. US Dept. of the Interior, Bureau of Reclamation, Technical Services Center, Denver, CO.

Bürger, G., Schulla, J., Werner, A.T., 2011. Estimates of future flow, including extremes, of the Columbia River headwaters. Water Resour. Res. 47, W10520. http://dx.doi.org/10.1029/2010WR009716.

Cayan, D.R., Tyree, M., Kunkel, K.E., Castro, C., Gershunov, A., Barsugli, J., Overpeck, J., Russell, J., Rajagopalan, B., Rangwala, I., Duffy, P., 2013. Future Climate: Projected Average. In: Garfin, G., Jardine, A., Merideth, R., Black, M., LeRoy, S. (Eds.), Assessment of Climate Change in the Southwest United States: A Report Prepared for the National Climate AssessmentA Report by the Southwest Climate Alliance. Island Press, Washington, D.C., pp. 101–125.

Chang, H., Jung, I.-W., 2010. Spatial and temporal changes in runoff caused by climate change in a complex large river basin in Oregon. J. Hydrol. 388 (3–4), 186–207. http://dx.doi.org/10.1016/j.jhydrol.2010.04.040.

Chen, J., Brissette, F.P., Chaumont, D., Braun, M., 2013. Performance and uncertainty evaluation of empirical downscaling methods in quantifying the climate change impacts on hydrology over two north American river basins. J. Hydrol. 479 (4), 200–214. http://dx.doi.org/10.1016/j.jhydrol.2012.11.062.

Cherkauer, K.A., Sinha, T., 2010. Hydrologic impacts of projected future climate change in the Lake Michigan region. J. Great Lakes Res. 36, 33–50. http://dx.doi.org/10.1016/j.jglr.2009.11.012.

Cherkauer, K.A., Bowling, L.C., Lettenmaier, D.P., 2003. Variable infiltration capacity cold land process model updates. Glob. Planet. Chang. 38 (1), 151–159. http://dx.doi.org/10.1016/S0921-8181(03)00025-0.

Chien, H., Yeh, P.J.-F., Knouft, J.H., 2013. Modeling the potential impacts of climate change on streamflow in agricultural watersheds of the Midwestern United States. J. Hydrol. 491, 73–88. http://dx.doi.org/10.1016/j.jhydrol.2013.03.026.

Christensen, N.S., Lettenmaier, D.P., 2007. A multimodel ensemble approach to assessment of climate change impacts on the hydrology and water resources of the Colorado River Basin. Hydrol. Earth Syst. Sci. 11 (4), 1417–1434. http://dx.doi.org/10.5194/hess-11-1417-2007.

Christensen, O.B., Gaertner, M.A., Prego, J.A., Polcher, J., 2001. Internal variability of regional climate models. Clim. Dyn. 17, 875–887. http://dx.doi.org/10.1007/s003820100154.

Christensen, N.S., Wood, A.W., Voisin, N., Lettenmaier, D.P., Palmer, R.N., 2004. The effects of climate change on the hydrology and water resources of the Colorado River basin. Clim. Chang. 62 (1–3), 337–363. http://dx.doi.org/10.1023/B:CLIM.0000013684.13621.1f.

Daly, C., Halbleib, M., Smith, J.I., Gibson, W.P., Doggett, M.K., Taylor, G.H., Curtis, J., Pasteris, P.P., 2008. Physiographically sensitive mapping of climatological temperature and precipitation across the conterminous United States. Int. J. Climatol. 28 (15), 2031–2064. http://dx.doi.org/10.1002/joc.1688.

Di Luca, A., de Elía, R., Laprise, R., 2012. Potential for added value in precipitation simulated by high-resolution nested regional climate models and observations. Clim. Dyn. 38 (5), 1229–1247. http://dx.doi.org/10.1007/s00382-011-1068-3.

Di Luca, A., de Elía, R., Laprise, R., 2013. Potential for small scale added value of RCM's downscaled climate change signal. Clim. Dyn. 40 (3–4), 601–618. http://dx.doi.org/10.1007/s00382-012-1415-z.

Diffenbaugh, N.S., Ashfaq, M., 2010. Intensification of hot extremes in the United States. Geophys. Res. Lett. 37, L15701. http://dx.doi.org/10.1029/2010GL043888.

Diffenbaugh, N.S., Pal, J.S., Trapp, R.J., Giorgi, F., 2005. Fine-scale processes regulate the response of extreme events to global climate change. Proc. Natl. Acad. Sci. U. S. A. 102 (44), 15,774–15,778. http://dx.doi.org/10.1073/pnas.0506042102.

Diffenbaugh, N.S., Ashfaq, M., Scherer, M., 2011. Transient regional climate change: analysis of the summer climate response in a high-resolution, century-scale ensemble experiment over the continental United States. J. Geophys. Res. 116, D24111. http://dx.doi.org/10.1029/2011JD016458.

Elguindi, N., Grundstein, A., 2013. An integrated approach to assessing 21st century climate change over the contiguous US using the NARCCAP RCM output. Clim. Chang. 117 (4), 809–827. http://dx.doi.org/10.1007/s10584-012-0552-z.

Environment Canada, 2014. HYDAT database. http://ec.gc.ca/rhc-wsc/default.asp?lang=En&n=9018B5EC-1 (accessed February 2014).

Ficklin, D.L., Stewart, I.T., Maurer, E.P., 2013. Climate change impacts on streamflow and subbasin-scale hydrology in the upper Colorado River basin. PLoS One 8 (8), e71297. http://dx.doi.org/10.1371/journal.pone.0071297.

Frumhoff, P.C., McCarthy, J.J., Melillo, J.M., Moser, S.C., Wuebbles, D.J., 2007. Confronting Climate Change in the U.S. Northeast: Science, Impacts, and Solutions. Synthesis Report of the Northeast Climate Impacts Assessment (NECIA). Union of Concerned Scientists (UCS), Cambridge, MA.

Garfin, G., Franco, G., Blanco, H., Comrie, A., Gonzalez, P., Piechota, T., Smyth, R., Waskom, R., 2014. Chapter 20: Southwest. Climate Change Impacts in the United States: The Third National Climate Assessment. U.S. Global Change Research Program, pp. 462–486.

Giorgi, F., Gutowski Jr., W.J., 2015. Regional dynamical downscaling and the CORDEX initiative. Annu. Rev. Environ. Resour. 40, 467–490. http://dx.doi.org/10.1146/annurev-environ-102014-021217.

Giorgi, F., Coppola, E., Solmon, F., Mariotti, L., Sylla, M.B., Bi, X., Elguindi, N., Diro, G.T., Nair, V., Giuliani, G., Turuncoglu, U.U., Cozzini, S., Güttler, I., O'Brien, T.A., Tawfik, A.B., Shalaby, A., Zakey, A.S., Steiner, A.L., Stordal, F., Sloan, L.C., Brankovic, C., 2012. RegCM4: model description and preliminary tests over multiple CORDEX domains. Clim. Res. 52, 7–29. http://dx.doi.org/10.3354/cr01018.

Glotter, M., Elliott, J., McInerney, D., Best, N., Foster, I., Moyer, E.J., 2014. Evaluating the utility of dynamical downscaling in agricultural impacts projections. Proc. Natl. Acad. Sci. U. S. A. 111 (24), 8776–8781. http://dx.doi.org/10.1073/pnas.1314787111.

Gordon, W.S., Famiglietti, J.S., 2004. Response of the water balance to climate change in the United States over the 20th and 21st centuries: results from the VEMAP phase 2 model intercomparisons. Glob. Biogeochem. Cycles 18, GB1030. http://dx.doi.org/10.1029/2003GB002098.

Goudie, A.S., 2006. Global warming and fluvial geomorphology. Geomorphology 79 (3–4), 384–394. http://dx.doi.org/10.1016/j.geomorph.2006.06.023.

Haddeland, I., Matheussen, B.V., Lettenmaier, D.P., 2002. Influence of spatial resolution on simulated streamflow in a macroscale hydrologic model. Water Resour. Res. 38 (7). http://dx.doi.org/10.1029/2001WR000854 (29–21–29-10).

Hagemann, S., Chen, C., Clark, D., Folwell, S., Gosling, S.N., Haddeland, I., Hannasaki, N., Heinke, J., Ludwig, F., Voss, F., Wiltshire, A.J., 2013. Climate change impact on available water resources obtained using multiple global climate and hydrology models. Earth Syst. Dyn. 4, 129–144. http://dx.doi.org/10.5194/esd-4-129-2013.

Hamlet, A.F., Lettenmaier, D.P., 1999. Effects of climate change on hydrology and water resources in the Columbia River basin. J. Am. Water Resour. Assoc. 35, 1597–1623. http://dx.doi.org/10.1111/j.1752-1688.1999.tb04240.x.

Hamlet, A.F., Elsner, M.M., Mauger, G.S., Lee, S.-Y., Tohver, I., Norheim, R.A., 2013. An overview of the Columbia Basin climate change scenarios project: approach, methods, and summary of key results. Atmosphere-Ocean 51 (4), 392–415. http://dx.doi.org/10.1080/07055900.2013.819555.

Harding, K.J., Snyder, P.K., Liess, S., 2013. Use of dynamical downscaling to improve the simulation of central US warm season precipitation in CMIP5 models. J. Geophys. Res. 118, 12,522–12,536. http://dx.doi.org/10.1002/2013JD019994.

Hay, L.E., Markstrom, S.L., Ward-Garrison, C., 2011. Watershed-scale response to climate change through the twenty-first century for selected basins across the United States. Earth Interact. 15, 1–37. http://dx.doi.org/10.1175/2010EI370.1.

Hayhoe, K., Wake, C.P., Huntington, T.G., Luo, L., Schwartz, M.D., Sheffield, J., Wood, E., Anderson, B., Bradbury, J., DeGaetano, A., Troy, T.J., Wolfe, D., 2007. Past and future changes in climate and hydrological indicators in the US northeast. Clim. Dyn. 28 (4), 381–407. http://dx.doi.org/10.1007/s00382-006-0187-8.

Hidalgo, H., Das, T., Dettinger, M.D., Cayan, D.R., Pierce, D.W., Barnett, T.P., Bala, G., Mirin, A., Wood, A.W., Bonfils, C., Santer, B.D., Nozawa, T., 2009. Detection and attribution of streamflow timing changes to climate change in the western United States. J. Clim. 22 (13), 3838–3855. http://dx.doi.org/10.1175/2009JCLI2470.1.

Huntington, T.G., Richardson, A.D., McGuire, K.J., Hayhoe, K., 2009. Climate and hydrological changes in the northeastern United States: recent trends and implications for forested and aquatic ecosystems. Can. J. For. Res. 39 (2), 199–212. http://dx.doi.org/10.1139/X08-116.

Jerla, C., Prairie, J., Adams, P., 2012. Colorado River Basin Water Supply and Demand Study: Study Report. U.S. Department of Interior, Bureau of Reclamation.

Johnson, T., Butcher, J., Parker, A., Weaver, C., 2012. Investigating the sensitivity of U.S. streamflow and water quality to climate change: U.S. EPA global change research Program's 20 watersheds project. J. Water Resour. Plan. Manag. 138 (5), 453–464. http://dx.doi.org/10.1061/(ASCE)WR.1943–5452.0000175.

Karl, T.R., Melillo, J.M., Peterson, T.C. (Eds.), 2009. Global Climate Change Impacts in the United States. Cambridge University Press, New York, NY.

Klos, P.Z., Link, T.E., Abatzoglou, J.T., 2014. Extent of the rain-snow transition zone in the western U.S. under historic and projected climate. Geophys. Res. Lett. 41, 4560–4568. http://dx.doi.org/10.1002/2014GL060500.

Knox, J.C., 1993. Large increases in flood magnitude in response to modest changes in climate. Nature 361, 430–432. http://dx.doi.org/10.1038/361430a0.

Kunkel, K.E., Liang, X.-Z., Zhu, J., 2010. Regional climate model projections and uncertainties of US summer heat waves. J. Clim. 23 (16), 4447–4458. http://dx.doi.org/10.1175/2010JCLI3349.1.

Kunkel, K.E., Karl, T.R., Brooks, H., Kossin, J., Lawrimore, J.H., Arndt, D., Bosart, L., Changnon, D., Cutter, S.L., Doesken, N., Emanuel, K., Groisman, P.Y., Katz, R.W., Knutson, T., O'Brien, J., Paciorek, C.J., Peterson, T.C., Redmond, K., Robinson, D., Trapp, J., Vose, R., Weaver, S., Wehner, M., Wolter, K., Wuebbles, D., 2013. Monitoring and understanding trends in extreme storms: state of knowledge. Bull. Am. Meteorol. Soc. 94 (4), 499–514. http://dx.doi.org/10.1175/BAMS-D-11-00262.1.

Lettenmaier, D.P., Wood, A.W., Palmer, R.N., Wood, E.F., Stakhiv, E.Z., 1999. Water resources implications of global warming: a U.S. regional perspective. Clim. Chang. 43 (3), 537–579. http://dx.doi.org/10.1023/A:1005448007910.

Liang, X., Lettenmaier, D.P., Wood, E.F., Burges, S.J., 1994. A simple hydrologically based model of land surface water and energy fluxes for general circulation models. J. Geophys. Res. 99 (D7), 14415–14428. http://dx.doi.org/10.1029/94JD00483.

Liang, X., Wood, E.F., Lettenmaier, D.P., 1996. Surface soil moisture parameterization of the VIC-2 L model: evaluation and modification. Glob. Planet. Chang. 13 (1), 195–206. http://dx.doi.org/10.1016/0921-8181(95)00046-1.

Liu, L., Hong, Y., Hocker, J.E., Shafer, M.A., Carter, L.M., Gourley, J.J., Bednarczyk, C.N., Yong, B., Adhikari, P., 2012. Analyzing projected changes and trends of temperature and precipitation in the southern USA from 16 downscaled global climate models. Theor. Appl. Climatol. 109 (3–4), 345–360. http://dx.doi.org/10.1007/s00704-011-0567-9.

Livneh, B., Rosenberg, E.A., Lin, C., Nijssen, B., Mishra, V., Andreadis, K.M., Maurer, E.P., Lettenmaier, D.P., 2013. A long-term hydrologically based dataset of land surface fluxes and states for the conterminous United States: update and extensions. J. Clim. 26, 9384–9392. http://dx.doi.org/10.1175/JCLI-D-12-00508.1.

Livneh, B., Bohn, T.J., Pierce, D.W., Munoz-Arriola, F., Nijssen, B., Vose, R., Cayan, D.R., Brekke, L., 2015. A spatially comprehensive, hydrometeorological data set for Mexico, the U.S., and southern Canada 1950–2013. Sci. Data 2, 150042. http://dx.doi.org/10.1038/sdata.2015.42.

Llewellyn, D., Vaddey, S., 2013. West-Wide Climate Risk Assessment: Upper Rio Grande Impact Assessment Report. US Department of the Interior, Bureau of Reclamation, Upper Colorado Region, Albuquerque Area Office.

Loukas, A., Vasiliades, L., Dalezios, N.R., 2002. Potential climate change impacts on flood producing mechanisms in southern British Columbia, Canada using the CGCMA1 simulation results. J. Hydrol. 259 (1–4), 163–188. http://dx.doi.org/10.1016/S0022-1694(01)00580-7.

Mahoney, K., Alexander, M.A., Thompson, G., Barsugli, J.J., Scott, J.D., 2012. Changes in hail and flood risk in high-resolution simulations over Colorado's mountains. Nat. Clim. Chang. 2 (2), 125–131. http://dx.doi.org/10.1038/nclimate1344.

Mallakpour, I., Villarini, G., 2015. The changing nature of flooding across the Central United States. Nat. Clim. Chang. 5 (3), 250–254. http://dx.doi.org/10.1038/nclimate2516.

Mankin, J.S., Diffenbaugh, N.S., 2014. Influence of temperature and precipitation variability on near-term snow trends. Clim. Dyn. 45 (3), 1099–1116. http://dx.doi.org/10.1007/s00382-014-2357-4.

Matonse, A.H., Pierson, D.C., Frei, A., Zion, M.S., Schneiderman, E.M., Anandhi, A., Mukundan, R., Pradhanang, S.M., 2011. Effects of changes in snow pattern and the timing of runoff on NYC water supply system. Hydrol. Process. 25, 3278–3288. http://dx.doi.org/10.1002/hyp.8121.

Maurer, E.P., 2007. Uncertainty in hydrologic impacts of climate change in the sierra Nevada, California, under two emissions scenarios. Clim. Chang. 82 (3–4), 309–325. http://dx.doi.org/10.1007/s10584-006-9180-9.

Maurer, E.P., Duffy, P.B., 2005. Uncertainty in projections of streamflow changes due to climate change in California. Geophys. Res. Lett. 32 (3). http://dx.doi.org/10.1029/2004GL021462.

Maurer, E.P., Wood, A.W., Adam, J.C., Lettenmaier, D.P., Nijssen, B., 2002. A long-term hydrologically based dataset of land surface fluxes and states for the conterminous United States. J. Clim. 15 (22), 3237–3251. http://dx.doi.org/10.1175/1520-0442(2002)015<3237:ALTHBD>2.0.CO;2.

Maurer, E.P., Hidalgo, H.G., Das, T., Dettinger, M.D., Cayan, D.R., 2010. The utility of daily large-scale climate data in the assessment of climate change impacts on daily streamflow in California. Hydrol. Earth Syst. Sci. 14, 1125–1138. http://dx.doi.org/10.5194/hess-14-1125-2010.

Mearns, L.O., Arritt, R., Biner, S., Bukovsky, M.S., McGinnis, S., Sain, S., Caya, D., Correia, J., Flory, D., Gutowski, W., Takle, E.S., Jones, R., Leung, R., Moufouma-Okia, W., McDaniel, L., Nunes, A.M.B., Qian, Y., Roads, J., Sloan, L., Snyder, M., 2012. The north American regional climate change assessment program: overview of phase I results. Bull. Am. Meteorol. Soc. 93, 1337–1362. http://dx.doi.org/10.1175/BAMS-D-11-00223.1.

Mearns, L.O., Sain, S., Leung, L.R., Bukovsky, M.S., McGinnis, S., Biner, S., Caya, D., Arritt, R.W., Gutowski, W., Takle, E., Snyder, M., Jones, R.G., Nunes, A.M.B., Tucker, S., Herzmann, D., McDaniel, L., Sloan, L., 2013. Climate change projections of the north American regional climate change assessment program (NARCCAP). Clim. Chang. 120 (4), 965–975. http://dx.doi.org/10.1007/s10584-013-0831-3.

Melillo, J.M., Richmond, T.T., Yohe, G. (Eds.), 2014. Climate Change Impacts in the United States: The Third National Climate Assessment. US Global Change Research Program http://dx.doi.org/10.7930/J0Z31WJ2.

Milly, P.C.D., Dunne, K.A., Vecchia, A.V., 2005. Global pattern of trends in streamflow and water availability in a changing climate. Nature 438, 347–350. http://dx.doi.org/10.1038/nature04312.

Mote, P.W., 2006. Climate-driven variability and trends in mountain snowpack in western North America. J. Clim. 19 (23), 6209–6220. http://dx.doi.org/10.1175/JCLI3971.1.

Mote, P.W., Parson, E.A., Hamlet, A.F., Keeton, W.S., Lettenmaier, D., Mantua, N., Miles, E.L., Peterson, D.W., Peterson, D.L., Slaughter, R., 2003. Preparing for climatic change: the water, salmon, and forests of the Pacific northwest. Clim. Chang. 61 (1–2), 45–88. http://dx.doi.org/10.1023/A:1026302914358.

Mote, P.W., Hamlet, A.F., Clark, M.P., Lettenmaier, D.P., 2005. Declining mountain snowpack in western North America. Bull. Am. Meteorol. Soc. 86 (1), 39–49. http://dx.doi.org/10.1175/BAMS-86-1-39.

Muerth, M.J., Gauvin St-Denis, B., Ricard, S., Velazquez, J.A., Schmid, J., Minville, M., Caya, D., Chaumont, D., Ludwig, R., Turcotte, R., 2013. On the need for bias correction in regional climate scenarios to assess climate change impacts on river runoff. Hydrol. Earth Syst. Sci. 17 (3), 1189–1204. http://dx.doi.org/10.5194/hess-17-1189-2013.

Myneni, R.B., Ramakrishna, R., Nemani, R., Running, S.W., 1997. Estimation of global leaf area index and absorbed PAR using radiative transfer models. IEEE Trans. Geosci. Remote Sens. 35 (6), 1380–1393. http://dx.doi.org/10.1109/36.649788.

Narisma, G.T., Foley, J.A., Licker, R., Ramankutty, N., 2007. Abrupt changes in rainfall during the twentieth century. Geophys. Res. Lett. 34, L06710. http://dx.doi.org/10.1029/2006GL028628.

Nash, L.L., Gleick, P.H., 1991. Sensitivity of streamflow in the Colorado basin to climatic changes. J. Hydrol. 125 (3–4), 221–241. http://dx.doi.org/10.1016/0022-1694(91)90030-L.

Nijssen, B., O'Donnell, G.M., Lettenmaier, D.P., Lohmann, D., Wood, E.F., 2001. Predicting the discharge of global rivers. J. Clim. 14 (15), 3307–3323. http://dx.doi.org/10.1175/1520-0442(2001)014<3307:PTDOGR>2.0.CO;2.

Notaro, M., Lorenz, D., Hoving, C., Schummer, M., 2014. Twenty-first-century projections of snowfall and winter severity across central-eastern North America. J. Clim. 27, 6526–6550. http://dx.doi.org/10.1175/JCLI-D-13-00520.1.

Ojima, D., Steiner, J., McNeeley, S., Cozetto, K., Childress, A., 2013. Great Plains Regional Climate Assessment Technical Report. National Climate Assessment 2013. Island Press.

Oubeidillah, A.A., Kao, S.-C., Ashfaq, M., Naz, B.S., Tootle, G., 2014. A large-scale, high-resolution hydrological model parameter data set for climate change impact assessment for the conterminous US. Hydrol. Earth Syst. Sci. 18 (1), 67–84. http://dx.doi.org/10.5194/hess-18-67-2014.

Pan, M., Sheffield, J., Wood, E.F., Mitchell, K.E., Houser, P.R., Schaake, J.C., Robock, A., Lohmann, D., Cosgrove, B., Duan, Q., Luo, L., Higgins, R.W., Pinker, R.T., Tarpley, J.D., 2003. Snow process modeling in the north American land data assimilation system (NLDAS): 2. Evaluation of model simulated snow water equivalent. J. Geophys. Res. 108, 8850. http://dx.doi.org/10.1029/2003JD003994.

Payne, J.T., Wood, A.W., Hamlet, A.F., Palmer, R.N., Lettenmaier, D.P., 2004. Mitigating the effects of climate change on the water resources of the Columbia River basin. Clim. Chang. 62 (1–3), 233–256. http://dx.doi.org/10.1023/B:CLIM.0000013694.18154.d6.

Peters, G.P., Andrew, R.M., Boden, T., Canadell, J.G., Ciais, P., Le Quéré, C., Marland, G., Raupach, M.R., Wilson, C., 2013. The challenge to keep global warming below 2 °C. Nat. Clim. Chang. 3 (1), 4–6. http://dx.doi.org/10.1038/nclimate1783.

Pradhanang, S.M., Frei, A., Zion, M., Schneiderman, E.M., Steenhuis, T.S., Pierson, D., 2013. Rain-on-snow runoff events in New York. Hydrol. Process. 27 (21), 3035–3049. http://dx.doi.org/10.1002/hyp.9864.

Prudhomme, C., Parry, S., Hannaford, J., Clark, D.B., Hagemann, S., Voss, F., 2011. How well do large-scale models reproduce regional hydrological extremes in Europe? J. Hydrometeorol. 12 (6), 1181–1204. http://dx.doi.org/10.1175/2011JHM1387.1.

Qiao, L., Hong, Y., McPherson, R., Shafer, M., Gade, D., Williams, D., Chen, S., Lilly, D., 2014. Climate change and hydrological response in the trans-state Oologah Lake watershed–evaluating dynamically downscaled NARCCAP and statistically downscaled CMIP3 simulations with VIC model. Water Resour. Manag. 28 (10), 3291–3305. http://dx.doi.org/10.1007/s11269-014-0678-z.

Rasmussen, R., Ikeda, K., Liu, C., Gochis, D., Clark, M., Dai, A., Gutmann, E., Dudhia, J., Chen, F., Barlage, M., Yates, D., Zhang, G., 2014. Climate change impacts on the water balance of the Colorado headwaters: high-resolution regional climate model simulations. J. Hydrometeorol. 15 (3), 1091–1116. http://dx.doi.org/10.1175/JHM-D-13-0118.1.

Reclamation (Bureau of Reclamation), 2012. St. Mary River and Milk River Basins Study Technical Report. Milk River Project, Montana Great Plains Region, U.S. Department of the Interior, Bureau of Reclamation.

Rojas, R., Feyen, L., Dosio, A., Bavera, D., 2011. Improving pan-European hydrological simulation of extreme events through statistical bias correction of RCM-driven climate simulations. Hydrol. Earth Syst. Sci. 15, 2599–2620. http://dx.doi.org/10.5194/hess-15-2599-2011.

Rosenberg, N.J., Brown, R.A., Izaurralde, R.C., Thomson, A.M., 2003. Integrated assessment of Hadley Centre (HadCM2) climate change projections on agricultural productivity and irrigation water supply in the conterminous United States: I. Climate change scenarios and impacts on irrigation water supply simulated with the HUMUS model. Agric. For. Meteorol. 117 (1), 73–96. http://dx.doi.org/10.1016/S0168-1923(03)00025-X.

Seager, R., Vecchi, G.A., 2010. Greenhouse warming and the 21st century hydroclimate of southwestern North America. Proc. Natl. Acad. Sci. U. S. A. 107 (50), 21277–21282. http://dx.doi.org/10.1073/pnas.0910856107.

Seager, R., Ting, M., Held, I., Kushnir, Y., Lu, J., Vecchi, G., Huang, H.-P., Harnik, N., Leetmaa, A., Lau, N.-C., Li, C., Velez, J., Naik, N., 2007. Model projections of an imminent transition to a more arid climate in southwestern North America. Science 316 (5828), 1181–1184. http://dx.doi.org/10.1126/science.1139601.

Seager, R., Ting, M., Li, C., Naik, N., Cook, B., Nakamura, J., Liu, H., 2013. Projections of declining surface-water availability for the southwestern United States. Nat. Clim. Chang. 3 (5), 482–486. http://dx.doi.org/10.1038/nclimate1787.

Sheffield, J., Pan, M., Wood, E.F., Mitchell, K.E., Houser, P.R., Schaake, J.C., Robock, A., Lohmann, D., Cosgrove, B., Duan, Q., Luo, L., Higgins, R.W., Pinker, R.T., Tarpley, J.D., Ramsay, B.H., 2003. Snow process modeling in the north American land data assimilation system (NLDAS): 1. Evaluation of model-simulated snow cover extent. J. Geophys. Res. 108, 8849. http://dx.doi.org/10.1029/2002JD003274.

Shrestha, R.R., Peters, D.L., Schnorbus, M.A., 2014. Evaluating the ability of a hydrologic model to replicate hydro-ecologically relevant indicators. Hydrol. Process. 28, 4294–4310. http://dx.doi.org/10.1002/hyp.9997.

Sinha, T., Cherkauer, K.A., 2010. Impacts of future climate change on soil frost in the midwestern United States. J. Geophys. Res. 115, D08105. http://dx.doi.org/10.1029/2009JD012188.

Stagge, J.H., Moglen, G.E., 2013. A nonparametric stochastic method for generating daily climate-adjusted streamflows. Water Resour. Res. 49, 6179–6193. http://dx.doi.org/10.1002/wrcr.20448.

Stewart, I.T., Cayan, D.R., Dettinger, M.D., 2004. Changes in snowmelt runoff timing in western North America under a 'business as usual' climate change scenario. Clim. Chang. 62 (1–3), 217–232. http://dx.doi.org/10.1023/B:CLIM.0000013702.22656.e8.

Stewart, I.T., Cayan, D.R., Dettinger, M.D., 2005. Changes toward earlier streamflow timing across western North America. J. Clim. 18 (8), 1136–1155. http://dx.doi.org/10.1175/JCLI3321.1.
Strzepek, K., Yohe, G., Neumann, J., Boehlert, B., 2010. Characterizing changes in drought risk for the United States from climate change. Environ. Res. Lett. 5 (4), 044012. http://dx.doi.org/10.1088/1748-9326/5/4/044012.
Takle, E.S., Jha, M., Lu, E., Arritt, R.W., Gutowski, W.J., 2010. Streamflow in the upper Mississippi river basin as simulated by SWAT driven by 20th century contemporary results of global climate models and NARCCAP regional climate models. Meteorol. Z. 19 (4), 341–346. http://dx.doi.org/10.1127/0941-2948/2010/0464.
Thomson, A.M., Brown, R.A., Rosenberg, N.J., Izaurralde, R.C., Benson, V., 2005. Climate Change Impacts for the Conterminous USA: An Integrated Assessment. In: Rosenberg, N.J., Edmonds, J.A. (Eds.), Climate Change Impacts for the Conterminous USA. Springer, pp. 43–65 http://dx.doi.org/10.1007/1–4020-3876-3_4.
Thornton, P.E., Running, S.W., White, M.A., 1997. Generating surfaces of daily meteorological variables over large regions of complex terrain. J. Hydrol. 190, 214–251. http://dx.doi.org/10.1016/S0022-1694(96)03128-9.
Tian, X., Dai, A., Yang, D., Xie, Z., 2007. Effects of precipitation-bias corrections on surface hydrology over northern latitudes. J. Geophys. Res. 112, D14101. http://dx.doi.org/10.1029/2007JD008420.
Tohver, I.M., Hamlet, A.F., Lee, S.Y., 2014. Impacts of 21st-century climate change on hydrologic extremes in the Pacific northwest region of North America. J. Am. Water Resour. Assoc. 50 (6), 1461–1476. http://dx.doi.org/10.1111/jawr.12199.
Vano, J.A., Udall, B., Cayan, D.R., Overpeck, J.T., Brekke, L.D., Das, T., Hartmann, H.C., Hidalgo, H.G., Hoerling, M., McCabe, G.J., Morino, K., Webb, R.S., Werner, K., Lettenmaier, D.P., 2014. Understanding uncertainties in future Colorado River streamflow. Bull. Am. Meteorol. Soc. 95 (1), 59–78. http://dx.doi.org/10.1175/BAMS-D-12-00228.1.
Vetter, T., Huang, S., Aich, V., Yang, T., Wang, X., Krysanova, V., Hattermann, F., 2015. Multi-model climate impact assessment and intercomparison for three large-scale river basins on three continents. Earth Syst. Dyn. 6 (1), 17–43. http://dx.doi.org/10.5194/esd-6-17-2015.
Wolock, D.M., McCabe, G.J., 1999. Explaining spatial variability in mean annual runoff in the conterminous United States. Clim. Res. 11 (2), 149–159.
Wood, A.W., Leung, L.R., Sridhar, V., Lettenmaier, D.P., 2004. Hydrologic implications of dynamical and statistical approaches to downscaling climate model outputs. Clim. Chang. 62, 189–216. http://dx.doi.org/10.1023/B:CLIM.0000013685.99609.9e.
Wood, E.F., Roundy, J.K., Troy, T.J., Van Beek, L., Bierkens, M.F., Blyth, E., de Roo, A., Döll, P., Ek, M., Famiglietti, J., Gochis, D., van de Giesen, N., Houser, P., Jaffé, P.R., Kollet, S., Lehner, B., Lettenmaier, D.P., Peters-Lidard, C., Sivapalan, M., Sheffield, J., Wade, A., Whitehead, P., 2011. Hyperresolution global land surface modeling: meeting a grand challenge for monitoring Earth's terrestrial water. Water Resour. Res. 47, W05301. http://dx.doi.org/10.1029/2010WR010090.
Wuebbles, D.J., Hayhoe, K., 2004. Climate change projections for the United States Midwest. Mitig. Adapt. Strateg. Glob. Chang. 9 (4), 335–363. http://dx.doi.org/10.1023/B:MITI.0000038843.73424.de.
Zhang, H., Huang, G.H., Wang, D., Zhang, X., 2011. Uncertainty assessment of climate change impacts on the hydrology of small prairie wetlands. J. Hydrol. 396 (1–2), 94–103. http://dx.doi.org/10.1016/j.jhydrol.2010.10.037.